Characterization of the Role of Mcm10 in DNA Replication in *Drosophila melanogaster*

by

Ritu Dalia

Director: Dr. Tim W. Christensen

Replication of the genome and proper formation, and packaging, of chromatin are processes essential to eukaryotic life. Maintenance of epigenetic chromatin states is essential for faithfully reproducing the transcriptional state of the cell; likewise, replication of DNA with high fidelity is crucial for accurate passage of genetic information from a cell to its progeny. Defects in DNA replication and improper regulation of the chromatin states can result in genome instability which can manifest as disease, or death of the organism. There are a plethora of factors involved in the process of DNA replication in eukaryotes, and recent studies have shed light on one of the factors called mini-chromosome maintenance 10 (Mcm10) as an essential DNA replication factor. First discovered in *S. cerevisiae*, Mcm10 is an abundant nuclear protein that has been implicated in the activation of the Pre-RC, interacts with members of the elongation machinery such as Polα, and has recently been shown to be required in the formation of heterochromatin in both yeast and Drosophila. Previous analysis of two Drosophila Mcm10 mutant alleles demonstrated that Mcm10 not only plays a role in DNA replication, but also has a role in heterochromatic silencing and chromosome condensation. With *Drosophila melanogaster* as a model we further investigated the roles of Mcm10 by using a collection of over 20 missense mutations generated via a Tilling approach. Mitotic index data generated using brain cells of these mutant strains showed no delays in progression through M-phase of cell cycle. Interestingly though, several aberrant chromosomal phenotypes such as condensation defects, aneuploidy, anaphase bridge defects, separated sister chromatids and chromosome breaks, were observed in varying frequencies suggesting that Mcm10 is involved in maintaining genomic stability. Additionally, the Mcm10 mutant strains showed defects in endoreplication and packaging of DNA within the nuclei of salivary glands. By understanding the various roles of Mcm10 we can help elucidate the biological functions of this well conserved protein as well as provide information on the domains of the protein required for its different biological functions.

Characterization of the Role of Mcm10 in DNA Replication in *Drosophila melanogaster*

A Thesis

Presented to

The Faculty of the Department of Biology

East Carolina University

in Partial Fulfillment

of the Requirements for the Degree

Master of Science in Biology

By

Ritu Dalia

25th November, 2013

Principal Investigator: Dr. Tim Christensen

Characterization of the Role of Mcm10 in DNA Replication in *Drosophila melanogaster*

by

Ritu Dalia

APPROVED BY:

DIRECTOR OF THESIS: _____

Tim W. Christensen, Ph.D

COMMITTEE MEMBER: _____

Anthony Caperhart, Ph.D

COMMITTEE MEMBER: _____

Edward Stellwag, Ph.D

COMMITTEE MEMBER: _____

Eli G. Hvastkovs, Ph.D

CHAIR OF THE DEPARTMENT OF BIOLOGY: _____

Jeff McKinnon, Ph.D

DEAN OF THE GRADUATE SCHOOL:_____

Paul J Gemperline, Ph.D

ACKNOWLEDGEMENTS

First and foremost I would like to thank my family for their continued support and encouragement throughout my academic career, my parents, Rajnikant and Saroj Dalia, my sister, Bhumi Dalia, and my husband, Ravi Barot. I would like to thank Dr. Tim W. Christensen for giving me the opportunity to conduct research in his lab and for providing his continued guidance and support throughout my time at East Carolina University. I would like to thank my committee members, Dr. Anthony Capehart, Dr. Edward Stellwag and Dr. Eli G. Hvastkovs for all their feedback and suggestions for my research project. I would like to thank the members of the Christensen lab (past and present): Michael Reubens for providing all the clean Mcm10 mutant fly lines for my project, Divya Devdasan for teaching me experiments, Garrett Ransdell for maintaining my fly lines in my absence, and Jeff Chmielewski, Wayne Rummings and Nicholas Faulkner for their help in lab activities. I would like to thank Dr. Elizabeth Ables for her training and assistance in using the LSM 700 Microscope. I would like to thank Dr. Tom Fink for his assistance with microscopy work as well. I would also like to thank Dr. Jeff McKinnon, Dr. Terry West, the Department of Biology and the Biology Graduate Student Association for their support during my time at ECU.

TABLE OF CONTENTS

LIST OF FIGURES

LIST OF TABLES

LIST OF ABBREVIATIONS

aa…….Amino acid
Cdc6…….Cell division cycle 6
Cdc7……..Cell division cycle 7 related protein kinase
Cdc45…….Cell division cycle 45
CDK……..…Cyclin dependent kinase
Cdt1……cdc 10 dependent kinase
CMG……..……Cdc45-Mcm-GINS
Ctf4……..Chromosome transmission fidelity 4
CTD……C-terminal domain
DAPI……..……..4’,6-diamidino-2-phenyllindole
Dbf4…….protein DBF4 homolog A
DDK……..…Dbf4-dependant cdc7 kinase
D. melanogaster……*Drosophila melanogaster*
DNA……..……Deoxyribonucleic acid
Dpb11……..…DNA polymerase B 11
dsDNA……..double-stranded DNA
Dup……..…Double-parked protein
EdU…….Ethynyl deoxyuridine
G_0 phase……..……..Gap 0 phase
G_1 phase…….Gap 1 phase
G_2 phase……Gap 2 phase
GINS……..…….Go-ichi-ni-san
HP1……...Heterochromatin protein 1
HS…….High sensitivity

ID……..Internal domain

KCl…….Potassium chloride

KH_2PO_4……Potassium dihydrogen phosphate

Mcm2-7……..……Minichromosome maintenance proteins 2-7

Mcm10……...Minichromosome maintenance protein 10

ml……Milliliter

mM…….Millimolar

mm…….Millimeter

M phase…….Mitosis phase

µg…….Microgram

µl……..Microliter

µm……..….Micrometer

NaCl……Sodium chloride

Na_2HPO_4……..Disodium hydrogen phosphate

ng……..Nanogram

Nm……..……Newton meter

NTD……....N-terminal domain

ORC……..Origin Recognition Complex

PBS……..Phosphate Buffered Saline

PBX…….….Phosphate Buffered Saline with Triton-X

PCNA……...Proliferating Cell Nuclear Antigen

PCR……...…Polymerase Chain Reaction

PEG…….Polyethylene glycol

pg……...Picogram

PIP……..……PCNA interacting peptide

Pol-α……..……..DNA polymerase alpha (α)

Pol-δ……..DNA polymerase delta (δ)

Pol-ε……..……DNA polymerase epsilon (ε)
pre-RC……..…pre-Replicative Complex
RecQ4…….ATP-dependent DNA helicase Q4
RNA……...Ribonucleic acid
RNAi…….RNA interference
RPA……...Replication Protein A
rpm…….Revolutions per minute
S. cerevisiae…….*Saccharomyces cerevisiae*
Scim 19……..……Sensitized chromosome inheritance modifier 19
Sir2……...Silent information regulator 2
SIRT1……...Sir2 homolog in mammals
Sld2……...Synthetic lethal with dpb11 2
Sld3……...Synthetic lethal with dpb11 3
S phase…….…Synthesis phase
S. pombe……..…….*Schizosaccharomyces pombe*
ssDNA……...single-stranded DNA
WT…….Wild Type
ZnF1…….Zinc Finger 1
ZNF2……Zinc Finger 2

Characterization of the Role of Mcm10 in DNA Replication in *Drosophila melanogaster*

I – INTRODUCTION

DNA is one of the key elements required for the growth and survival of any living organism, which makes replication of the DNA a very crucial process. DNA replication occurs with very high fidelity to ensure that the genetic information can be passed to daughter cells in identical copies. Similarly, DNA packaging in a highly condensed state called chromatin is also very crucial since maintenance of the epigenetic chromatin states is key to maintaining the transcriptional states of the cell. These transcriptional states then dictate the behavior of a cell; whether it will be a cancer cell, or a stem cell or a differentiated cell. Thus both DNA replication and its proper packaging form the foundation of the proper cell behavior.

I. 1. Stages of a Cell Cycle

In order to understand the mechanisms involved in DNA replication it is essential to know when this event occurs during the cell cycle which is comprised of four phases: Gap1 (G_1), Synthesis (S), Gap2 (G_2) and Mitosis (M) **(Figure 1)**. When a cell is dormant it remains in the Gap 0 (G_0) phase, also known as the extended G_1 phase. In dividing cells the first phase is the G_1 phase where the cell accumulates nutrients to grow and prepare for the second phase called the Synthesis (S) phase. It is during the S-phase that DNA replication occurs. The S-phase is important in that mutation or other damage in DNA can have

unforeseen consequences on DNA replication. After the S phase, the cell enters the third phase known as the Gap2 (G_2) phase which is when the cell again builds up nutrients to proceed to the fourth phase called the Mitotic phase. The G_2 phase is hypothesized to be essential in controlling the cell size that is found to be aberrant in certain cancers **[Moseley *et al.*, 2009]**. Finally, the cell undergoes division during mitosis, which is when the replicated DNA is equally distributed and packaged into chromatin in the two daughter cells generated.

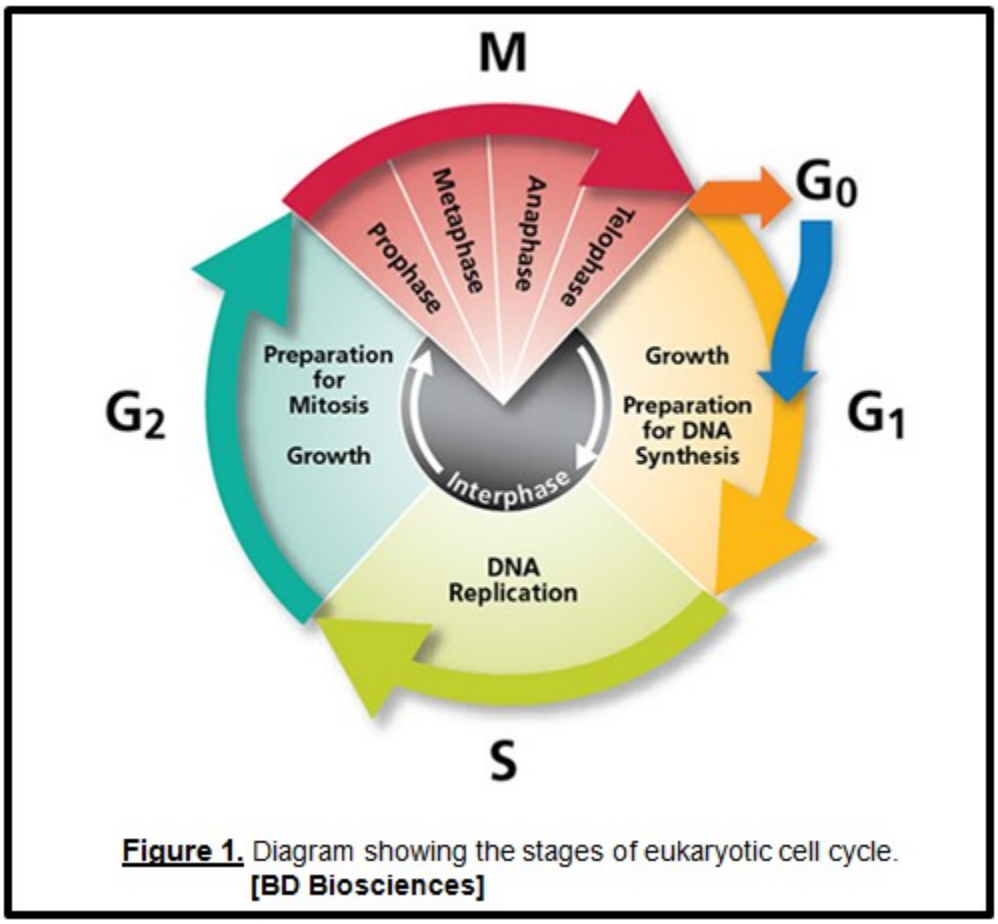

Figure 1. Diagram showing the stages of eukaryotic cell cycle. **[BD Biosciences]**

Five stages, namely, the prophase, prometaphase, metaphase, anaphase and telophase comprise the continuous M-phase of the cell cycle **(Figure 2)**. DNA begins to

condense at the end of G_2 phase, a process that continues during prophase. Additionally, prophase is marked by formation of spindle fibers that ultimately attach to the centromere of the sister chromatids during prometaphase. Metaphase is marked by alignment of the chromatids along the metaphase plate, an imaginary site located roughly in the middle of the mitotic nucleus. Following this the cell enters anaphase which is when the sister chromatids are partitioned by the formation of nuclear membrane that begins to divide the preexisting nucleus into separate nuclei through a process referred to as karyokinesis. In the final stage of mitosis the separated sister chromatids begin to decondense and become completely partitioned into two nuclei during telophase stage. Ultimately, the original mother cell divides by transverse fission through cytokinesis and the two newly formed daughter cells enter G_1 phase commencing the cell cycle all over again.

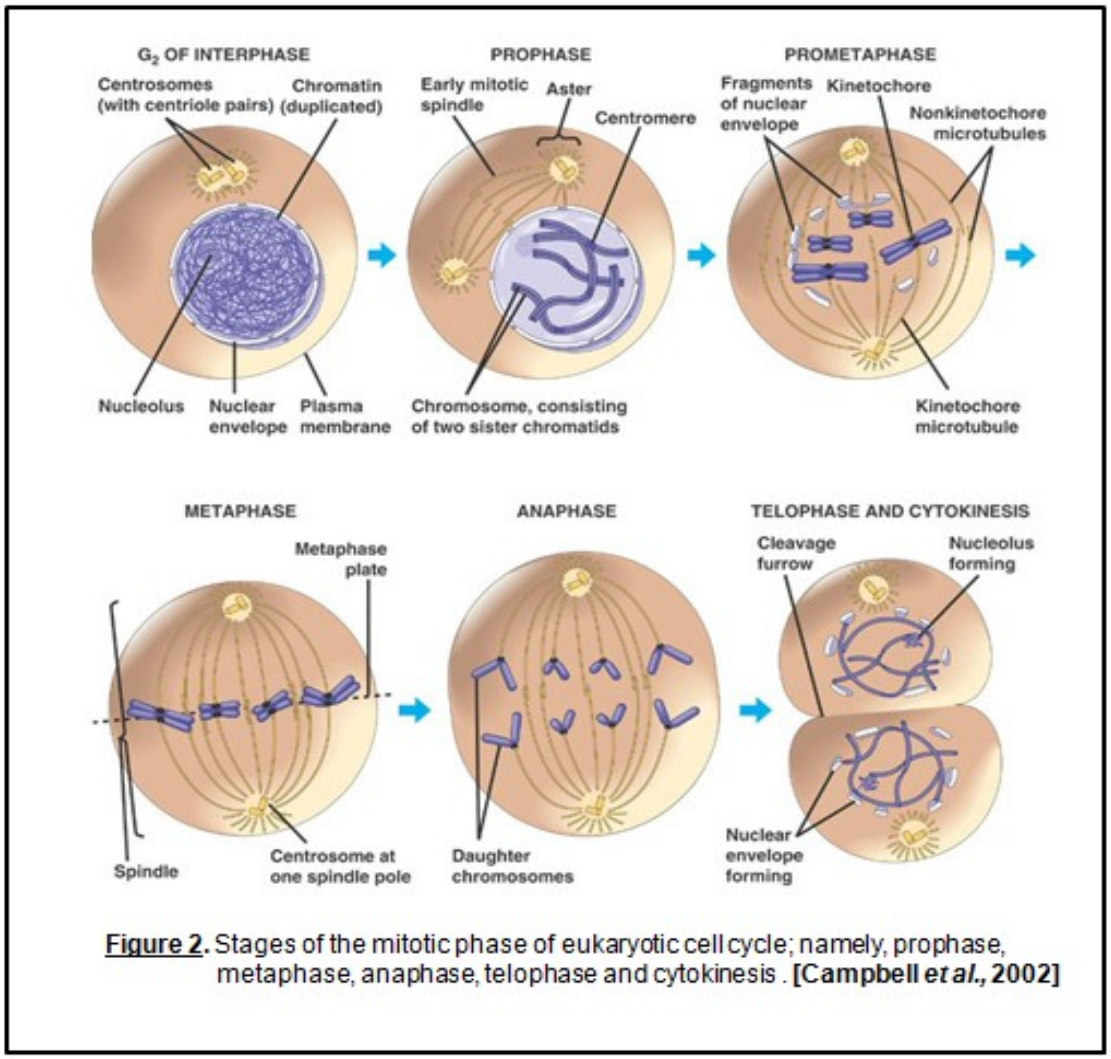

Figure 2. Stages of the mitotic phase of eukaryotic cell cycle; namely, prophase, metaphase, anaphase, telophase and cytokinesis . **[Campbell *et al.*, 2002]**

I. 2. DNA Replication

Two of the most important events in a cell's cycle are copying the chromosomal DNA during S-phase and accurately partitioning the genetic material into daughter cells during mitosis **[Nurse, 2000]**. The process of DNA replication can be divided into three crucial steps: initiation, elongation and termination **[Bell *et al.*, 2002].** For the sake of this thesis, I will be discussing the process of replication only in terms of recognition, licensing, and initiation.

In eukaryotic cells, assembly of a protein complex called the replisome commences in the G_1 phase in a highly controlled manner. This replisome machinery is responsible for the unwinding and the semi-conservative bi-directional replication of DNA. The highly coordinated process of replication initiates at multiple locations on the chromosomes called replication origins. These origins get recognized and bound by origin recognition complexes (ORCs 1- 6) **(Figure 3)**. The ORCs act as binding sites where two clamp loaders, cell division cycle 6 (cdc6) and cdc10 dependent transcript 1 (cdt1), then load the ring-shaped double hexameric helicase, minichromosome maintenance (Mcm) proteins Mcm 2-7 onto the chromatin in an ATP-dependent manner **[Remus *et al.*, 2009 and Machida Y *et al.*, 2005]**. Mcm 2-7 encircles the DNA duplex and remains inactive during the G_1 phase. Once this pre-replicative complex (pre-RC) has assembled on the ORCs the cell is considered "licensed" for DNA replication **[Sclafani *et al.,* 2007]**. This origin licensing ensures that DNA gets replicated only once during the cell cycle allowing only one S-phase for each cell cycle.

The G1-to-S-phase transition of the cell is triggered by the activation **(Figure 3)** of the pre-RC through phosphorylation of Mcm 2-7 helicase by cyclin-dependent kinase (CDK) and Dbf4-dependent kinase Cdc7 (DDK). In yeast, CDK phosphorylates Sld2 and Sld3 and facilitates their binding to Dpb11 **[Tanaka *et al.* 2007; Zegerman and Diffley 2007]** and DDK phosphorylates Mcm2 and Mcm4 **[Lei *et al*. 1997; Sheu and Stillman 2006].** One of the first proteins to be loaded onto the chromatin during the onset of S-phase is Mcm10 which is important for both activating Mcm 2-7 and recruiting other replisome proteins **[Wohlschlegel *et al.*, 2002]**. Mcm10 has been shown to stimulate phosphorylation of Mcm2-7 by DDK and may play a role in recruiting DDK to the pre-RC **[Lee *et al.* 2003]**. Activation of the Mcm complex leads to the recruitment of two helicase coactivators, Cdc45 and the GINS (go-inchi-

ni-san for 5-1-2-3 in Japanese) complex to form the pre-initiation complex (pre-IC). Together, Cdc45 - Mcm2-7 - GINS form the CMG complex which is the functional helicase that unwinds the DNA **[Moyer S.E. *et al.*, 2006]**. The precise unwinding of DNA is carefully timed and Mcm10 appears to be essential for this crucial step **[Wohlschlegel, J.A. *et al.* 2002; Kanke M. *et al.,* 2012; van Deursen, F. e*t al.,* 2012; Watase G. *et al.*, 2012]**. Next, single-stranded DNA (ssDNA) binding protein replication protein A (RPA) is recruited to the unwound origin and the replication initiation phase is concluded. Elongation of the DNA requires the synthesis machinery to begin fork firing. DNA polymerase α (Pol-α) – primase is needed to begin DNA synthesis by generating RNA primers and short stretches of DNA on both the leading and lagging strands. Mcm10 along with the cohesion protein And-1/Ctf4 have been implicated in loading Pol-α onto the chromatin and also facilitating its interaction with Mcm2-7 **[Gambus A. *et al.,* 2009; Im J.S. *et al.,* 2009; Lee e*t al.,* 2010; Ricke and Bielinsky 2004; Zhu e*t al.,* 2007]**. DNA polymerases δ and ε then processively synthesize DNA with the help of the sliding clamp, proliferating cell nuclear antigen (PCNA).

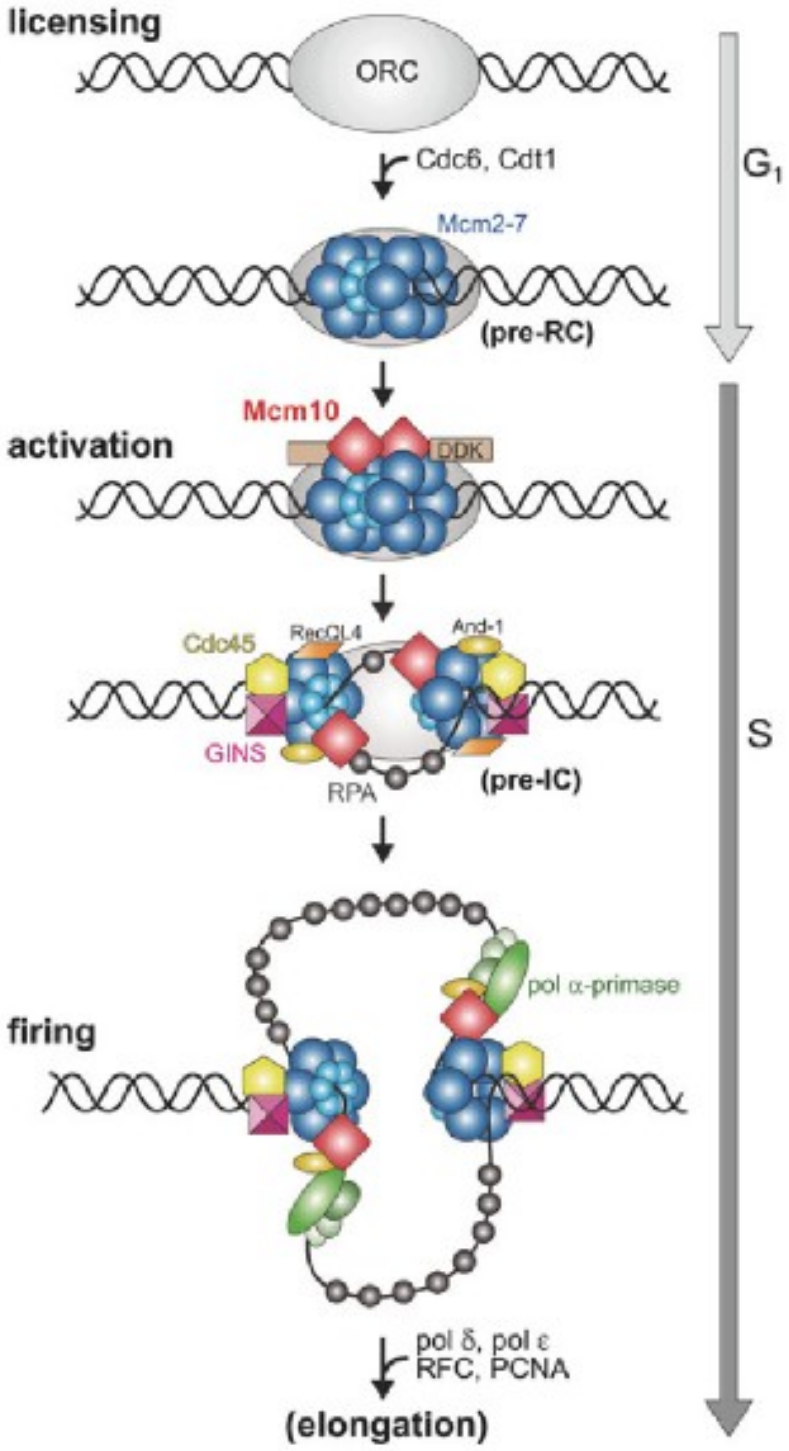

Figure 3. **Simplified view of the stages during initiation of DNA replication. [Du W. *et al.*, 2012].**

I. 3. Roles of Mcm10 in Replication

There are a plethora of factors involved in the process of DNA replication in eukaryotes. Recent studies have shed light on one of the essential DNA replication factors called mini-chromosome maintenance 10 (MCM10). Initially identified as a protein needed for the stable maintenance of mini-chromosomes in budding yeast *Saccharomyces cerevisiae* ***[Homesley et al.,2000 and Merchant et al., 1997],*** MCM10 is known to interact with members of the pre-initiation complex including MCM2-7, ORC, Cdc7 (Cell division cycle 7-related protein kinase), Dbf4 (protein DBF4 homolog A) and the GINS complex (composed of Sld5, Psf1, Psf2, and Psf3) **[Chmielewski J.P. *et al.,* 2012]**. Human Mcm10 (hMcm10) interacts with chromatin at the G_1/S – phase transition and dissociates in G_2 phase **[Izumi *et al.,* 2000]**. Studies in budding yeast indicate that Mcm10 stimulates phosphorylation of Mcm2-7 to activate the pre-RC **[Lee *et al.*, 2003].** Similar interactions of other Mcm10 orthologues with Mcm2-7 have been reported in *Drosophila* **[Apger *et al.,*2010]**, *Xenopus* **[Zhu *et al.,* 2007]**, and human **[Izumi *et al.,* 2000].** Mcm10 has also been shown to directly interact with the RecQ4 helicase and aids in its interaction with Mcm 2-7 **[Xu *et al.*, 2009]**.

Once the pre-RC has been activated in the S-phase, synthesis machinery is recruited to the replication fork. Replication firing requires loading of DNA polymerase (Pol-α) to begin elongation. Mcm10 along with And-1/Ct4 have been implicated in loading Pol-α on the chromatin and regulating its stability during replication **[Ricke RM *et al.,* 2004, 2006 and Wang *et al.*,2010]**. Mcm10 also guide's Pol-α's physical interaction with Mcm2-7 **[Zhu *et al.,* 2007]**.

Although studies have established that Mcm10 interacts with an array of other replication proteins, there are several discrepancies about how and when it conducts these interactions. For instance, initial studies in *S. cerevisiae*, *Schizosaccharomyces pombe* (S. pombe) and *Xenopus* egg extracts suggested that Mcm10 was loaded on chromatin after origin licensing but before initiation of replication **[Wohlschlegel J.A. *et al.,* 2002; Ricke and Bielinsky 2004; Gregan J. *et al.*, 2003]**. Some studies suggest that Mcm10 plays a role in the recruitment of the helicase coactivator Cdc45 **[Wohlschlegel J.A. *et al.,* 2002; Gregan J. *et al.*, 2003; Sawyer S.L. *et al.* 2004]** while other *in vitro* experiments in budding yeast whole cell extracts show that the CMG complex can be assembled in the absence of Mcm10 **[Heller *et al.,* 2011]**. There is debate in the literature about when Mcm10 gets loaded onto chromatin as well. Whether Mcm10 is loaded in late G_1 – phase or early S-phase could depend on whether Mcm10 loading requires DDK or CDK, respectively **[Thu Y.M. and Bielinsky 2013]**. Since Mcm10 can bind both ssDNA and double-stranded DNA (dsDNA) **[Eisenberg S. *et al.,* Fien K. *et al.* 2004; Robertson *et al.,* 2008, 2010; Warren E.M. *et al.,* 2008]**, both these scenarios seem possible. However, it is clear that Mcm10 loads onto chromatin at the G_1/S transition and it is around the same time as Cdc45 and GINS are recruited.

It is also established that Mcm10 is involved in unwinding of DNA replication origin during replication initiation in *Xenopus*, *S. cerevisiae, and S. pombe* **[Wohlschlegel J.A. *et al.,* 2002; Kanke M. *et al.,* 2012; van Deursen, F. e*t al.,* 2012; Watase G. *et al.*, 2012].** Mcm10's role in activating the helicase is subject of considerable interest in the field. CMG remodeling could be required to facilitate the transition of double hexamer Mcm2-7 on dsDNA to translocating as mono – hexamer on ssDNA **[Gambus A. *et al.*, 2006; Fu Y.V. *et al.,***

2011]. A recent study has for the first time shown a direct physical interaction between Mcm10 and Cdc45 which is part of the CMG complex **[Perna R.D, e*t* a*l,* 2013]**. This could suggest a more direct role of Mcm10 in unwinding DNA. Additionally, in higher eukaryotes Mcm10 interacts with RecQ4 helicase and regulates its function in an inhibitory manner **[Xu *et al.,* 2009].** Another possibility could also be that Mcm10 helps unwind the DNA indirectly by stabilizing ssDNA. However, the exact nature of Mcm10's role in CMG remodeling remains unclear.

Several studies suggest that Mcm10 migrates with the elongating replication fork by associating with DNA and DNA polymerases. Recruitment of both Pol-α and Pol-δ in *S.cerevisiae* is greatly reduced when Mcm10 is depleted **[Heller *et al.,* 2011]**. Mcm10 has also been shown to bind the catalytic subunit, p180, of Pol-α in human cells and is needed for Pol-α's association with chromatin **[Chattopadhyay and Bielinsky 2007]**. Mcm10 stabilizes Pol-α throughout the cell cycle by preventing its degradation by proteasome **[Chattopadhyay and Bielinsky 2007; Ricke and Bielinsky 2004, 2006; Yang *et al*., 2005]**.

I. 4. Structure of Mcm10

More insight into the functionality of Mcm10 depends on an understanding of its structure. Mcm10 was identified in the same genetic screens in yeast that yielded the first of the Mcm 2-7 proteins **[Merchant *et al.*, 1997]**. However, the primary DNA sequence of Mcm10 is not homologous to that of Mcm2-7 **[Liu *et al.,* 2009]** but Mcm10 is highly abundant and evolutionarily conserved in most eukaryotes **(Figure 4).** The size of Mcm10 ranges from 571 amino acids in yeast to 874 in humans with regions of homology found in the central and extreme N- and C- terminals **[Du W. *et al*., 2012]**. Figure 4 shows the functional homologs of

Mcm10 from various species where the central black region containing a zinc-finger is highly conserved and the gray regions show some conservation. Proteolysis and mass spectrometry studies show that the full length xMcm10 consists of three structured domains; the N-terminal domain (NTD), internal domain (ID) and the C-terminal domain (CTD) **[Robertson et al, 2008]**. The amino acid sequence alignment of Mcm10 from multiple eukaryotic species shows that both the NTD and the ID are conserved in the metazoans suggesting that these regions play a critical role. The CTD as shown in **figure 4** is unique to higher eukaryotes and this region of Mcm10 could have been acquired in metazoans after their divergence from a common eukaryotic ancestor or lost in the yeast after their divergence from their common ancestor with metazoans. This suggests that the CTD of Mcm10 could be required to conduct additional roles in higher eukaryotes that undergo many developmental changes throughout their life cycle as opposed to the simpler cell to cell growth of yeast.

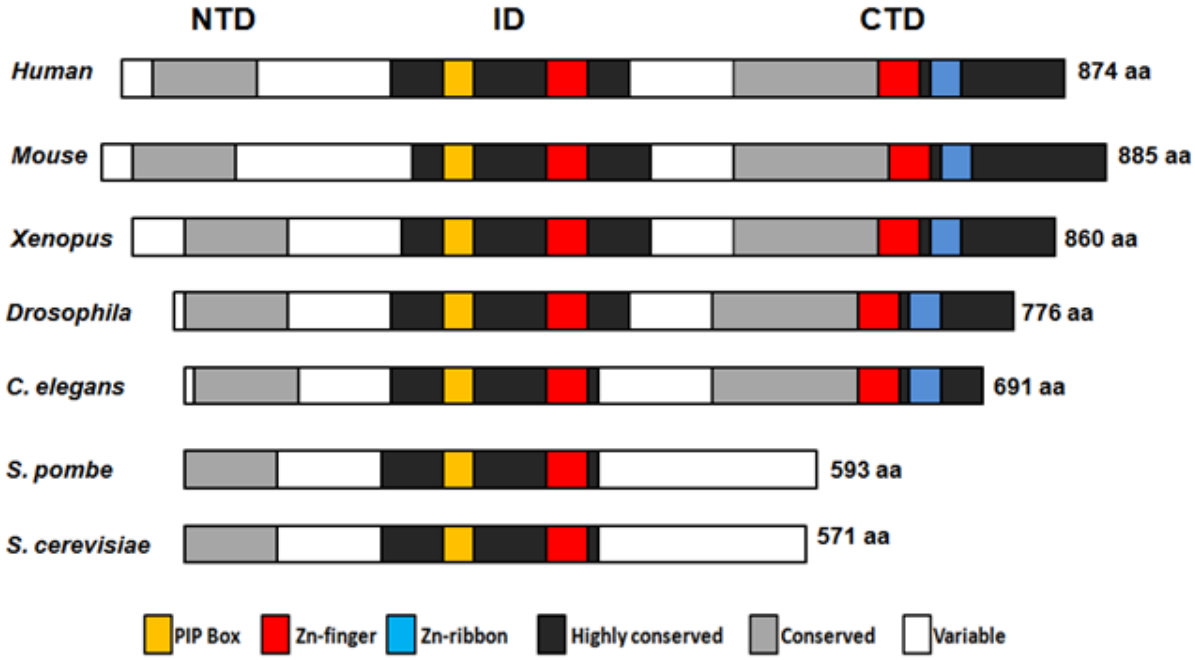

Figure 4. Amino acid sequence alignment of Mcm10 from multiple species with regions of high conservation in black and somewhat conserved in gray. PCNA interacting peptide (PIP) region (yellow), CCCH-type zinc finger (red) and CCCC-type zinc ribbon (blue).

Work from the Christensen laboratory reported a strong yeast one-hybrid interaction from the first 100 residues of *Drosophila* Mcm10 **[Apger *et al.*, 2010],** which suggests that the N-terminal domain (NTD) might function as an oligomerization domain for the full length protein. A recent study in *Xenopus* showed that Mcm10 self associates via a coiled-coil domain in its N-terminal **[Du W. *et al.,* 2013]**. The dimerization of NTD **(Figure 5c.)** could orient MCM10 in a manner that could facilitate its interaction with both the leading and lagging strands of DNA at the replication fork. There seems to be some controversy regarding the potential of Mcm10 to adopt an oligomeric structure. *S. cerevisiae* Mcm10 has

been shown to form large, 800kDa homocomplexes, as many as 12 molecules **[Cook C. R. *et al*., 2003]** while Mcm10 from *S. pombe* appears to be limited to only monomeric and dimeric forms **[Fien and Hurwitz 2006; Lee *et. al*., 2003]**. Electron microscopy of human Mcm10 reveals a homohexameric ring structure **(Figure 6)**, the dimensions of which would allow Mcm10 to physically surround DNA and act in a manner similar to the PCNA sliding clamp and facilitate interactions with other proteins in the pre-RC **[Okorokov *et al.,* 2007]**. The hexameric ring structure of Mcm10 resembles that of Mcm 2-7 proteins but lacks the helicase activity of Mcm 2-7. This suggests that Mcm10 may act as a scaffold protein that helps co-localize essential replication factors within the replisome during both the initiation and elongation stages of DNA replication **[Du W. *et al*., 2012]**.

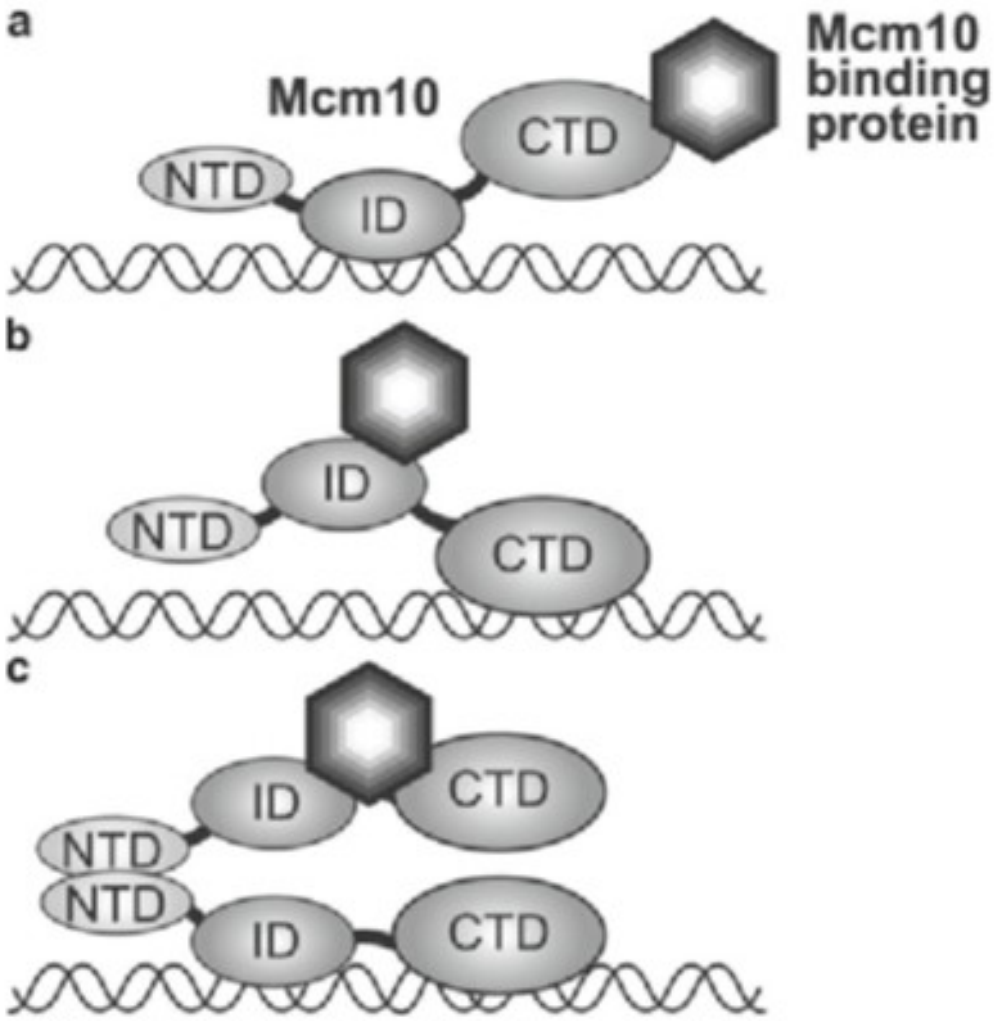

Figure 5. Schematic representing three possible models for Mcm10's interaction with DNA and other binding proteins (ex. Pol-α). **[Du W. *et al.*, 2012]**

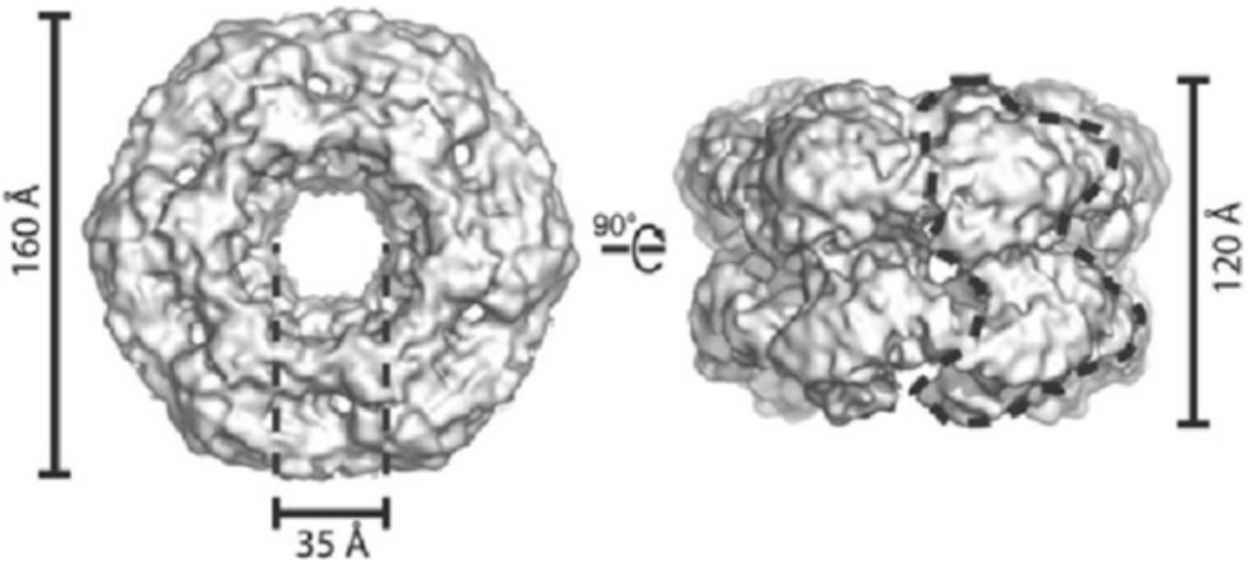

Figure 6. Structure of human Mcm10 as determined by electron microscopy and single-particle analysis. **[Du W. *et al.*, 2012]**

The internal domain is the most conserved region of Mcm10 across species from yeast to vertebrates **(Figure 4) [Izumi *et al.* 2000].** The internal domain consists of a CCCH-type zinc finger and an oligonucleotide/oligosaccharide binding (OB)-fold that are known to facilitate Mcm10's interactions with DNA and other proteins **[DU W. *et al.,* 2012]**. This domain has been specifically shown to interact with ssDNA and the N- terminal domain of Pol-α **[Robertson *et al.,* 2008]**. Additionally, mutations discovered from yeast genetic screens and those identified to disrupt scMcm10 association with PCNA and Pol-α, are all located in the ID **[Das- Bradoo e*t al.,* 2006; Ricke and Bielinksy 2006]**. PCNA interacts

with diubiquitinylated Mcm10 in budding yeast **[Das-Bradoo *et al.,* 2006]** and this region has been mapped to a PCNA interacting peptide (PIP) region in the ID of Mcm10 **(Figure 4).**

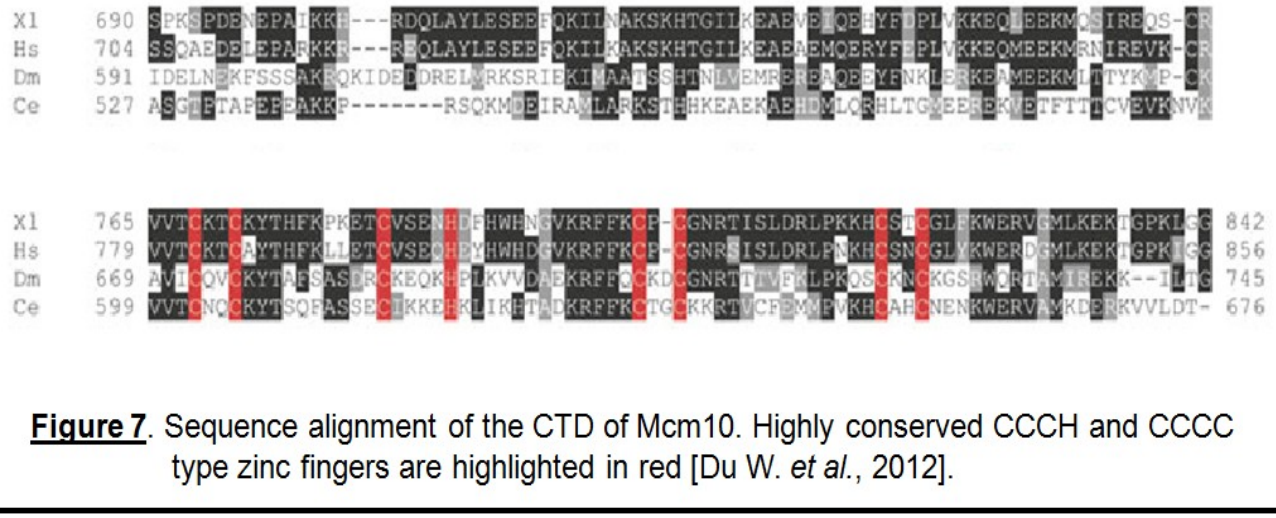

Figure 7. Sequence alignment of the CTD of Mcm10. Highly conserved CCCH and CCCC type zinc fingers are highlighted in red [Du W. *et al.*, 2012].

The CTD of Mcm10 is unique to higher eukaryotes **(Figure 4)** and consists of a highly conserved CCCH-type zinc finger (ZF1) and a CCCC-type zinc finger (ZF2) **(Figure 7)**. The CTD in *Xenopus* Mcm10 has been shown to bind ssDNA, dsDNA, and Pol-α **[Robertson et al., 2010]**. Recent work in Drosophila has shown that Mcm10 interacts directly with Mcm2 via its CTD **[Apger et al., 2010]**. Since both the ID and CTD can bind DNA, there could be multiple ways in which Mcm10 interacts with DNA and other binding proteins such as Pol-α. **Figures 5 a and b** are a schematic that represent models that show how the ID could bind DNA allowing the CTD to bind other proteins or how the CTD could bind DNA allowing the ID to interact with other proteins. *Xenopus* Mcm10 ID and CTD together have been shown to bind DNA with 10-fold greater affinity **[Robertson *et al., 2008;* Warren E.M. *et al.,* 2009]**

and the catalytic subunit of Pol-α with 15-fold greater affinity, than each domain alone **[Warren E.M. *et al.,* 2009].** The ZnF1 is shown to be the predominant DNA binding site in the CTD while the ZnF2 does not bind DNA **[Robertson *et al.,* 2010]**. Additionally, in a recent study it was shown that the direct physical interaction of Mcm10 with the helicase coactivator, Cdc45, occurs via its CTD **[Perna R.D. *et al.,* 2013]**. **Figure 8** shows a model representing the possible mechanism by which Mcm10 could be interacting with DNA and Cdc45. As shown in this model, Mcm10 binds to ssDNA via the ID and the ZnF1 of the CTD while the remainder of the CTD binds to Cdc45. This model seems to be consistent with the other Mcm10 interaction models presented in **figure 5**. There have been several genetic studies focusing on the role of the ID of Mcm10 but little work has been conducted on the CTD. Hence the CTD of Mcm10 is the focus of our research using *Drosophila* as the model organism, which will help shed some more light on its functions.

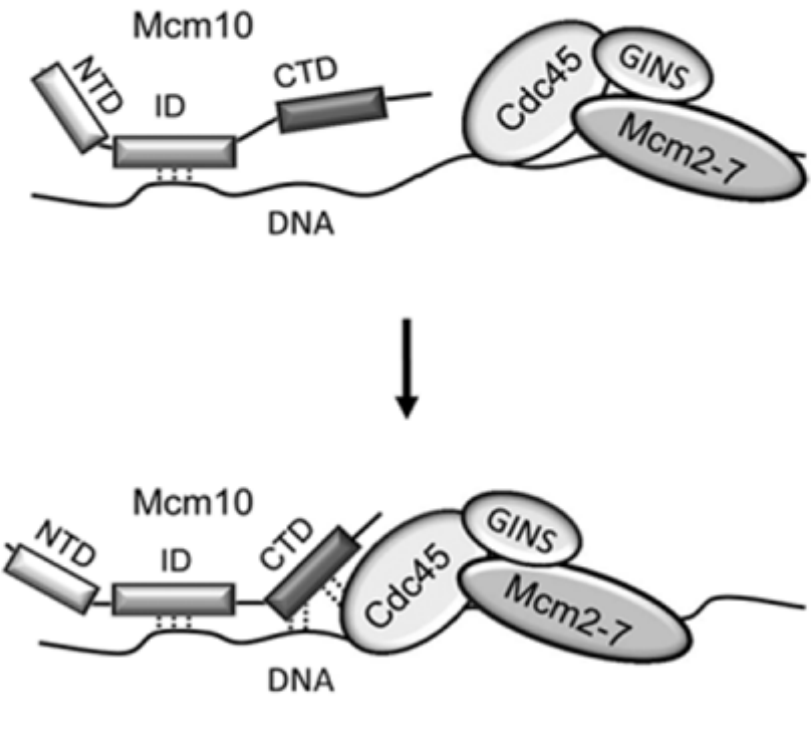

Figure 8. Schematic representation of Mcm10 recruitment to CMG on DNA **[Perna R. Di *et al.*, 2013]**.

I. 5. Endoreplication

Normal eukaryotic replication occurs in a highly controlled fashion only once per cell cycle, during the S-phase **(Figure 1)**. However, variation in the nature of the cell cycle and its relationship to the DNA replication cycle exist in different cell types of different. In cells like those of the ovarian, nurse, and follicle cells of larval tissues in flies and the placental giant tropoblasts and megakaryocytes in mammals that are polyploidy. Cells accumulate more than a diploid complement via endoreplication. Endoreplication is a cell cycle variation that generates a polyploidy genome by repeating rounds of DNA replication in the absence of

cell division. There are two forms of endoreplication, namely – endomitosis and endocycling **(Figure 9)**. During endomitosis cells enter but do not complete mitosis **(Figure 9B**), while endocycling cells lack M phase and consist of alternating S and G phases only. The research in this thesis is directed toward mechanisms related exclusively to endocycling.

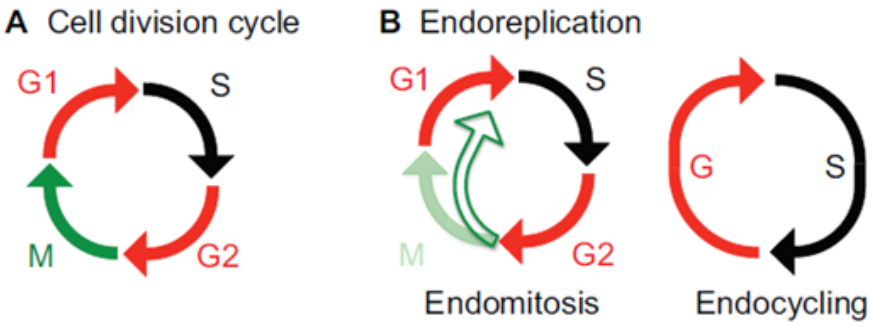

Figure .9 Schematic representation of the different replication cycles. **A.** Normal Cell cycle leading to one round of DNA replication. **B.** Endoreplication can occur either by endomitosis, a cell cycle that displays features of mitosis but lacks cytokinesis, or by endocycling in which periods of S and G phase alternate with no cell division. **[Fox D.T. & Duronio R. J., 2013]**

Endocycling is a widespread form of endoreplication, which is developmentally controlled and consists of discrete periods of S-phase and G-phase resulting in cells with a single polyploidy nucleus **[Edger and Orr-Weaver, 2001; Lily and Duronio, 2005]**. A key feature of the endocycle is that DNA content increases by delineated genome doubling. This is an important distinction from the aberrant process of rereplication which is uncontrolled continuous reinitiation of DNA synthesis within a given S-phase that does not lead to distinct genome doubling. Rereplication occurs when the molecular mechanisms controlling the once

and only once" firing of replication origins during S-phase are perturbed, leading to genomic instability, and is a phenomenon observed in many cancers **[Lee H.O. *et al.,* 2009]**.

Many organisms use endoreplication as part of terminal differentiation to generate a balanced increase in gene dosage above the diploid dose presumably to provide increased levels of metabolic enzymes to facilitate the acquisition of nutrients and provide a sufficient quantity of proteins to support the developing egg or embryo. For instance, in *Drosophila* females, endoreplication is essential for egg production. Sterility has been seen in nurse and follicle cells of *Drosophila* when endoreplication is reduced, suggesting that the endocycle plays an essential role in oogenesis and development **[Lily and Spradling, 1996; Maines e*t al.,* 2004].** Organisms grow either by increasing cell number as in normal cell division cycle or by increasing cell size as in endoreplication or both. Endoreplication provides a more efficient mechanism for growth in certain tissues as increasing cell volume consumes less energy than increasing cell surface area needed for cell division **[Kondorosi *et al.,* 2000]**. *Drosophila* and *Caenorhabditis elegans* larvae growth is mainly driven by endoreplication **[Edgar and Orr-Weaver, 2001].**

As discussed earlier, in order to maintain genomic integrity, proliferating cells have to duplicate the entire genome once, and only once, per cell division cycle. And this is ensured by the highly controlled and timed assembly of the pre-RC factors onto the origins in G_1 phase and initiation of synthesis during S-phase preventing any reinitiation leading to aberrant rereplication. Studies in *Drosophila* have shown that ORC, and MCM4 are dispensable for endoreplication **[Feger G. *et al.,*1995; Lake C.M. *et al.* 2007; Park S.Y. and Asano M., 2008]**. By contrast, double-parked protein (Dup)/Cdt1 and minichromosome maintenance proteins are essential for Endoreplication, which suggests that some

components of pre-RC involved in mitotic replication are also involved in initiation during endoreplication. To investigate whether Mcm10 has a role in endoreplication, salivary glands in *Drosophila* were used to see if any Mcm10 gene mutations resulted in chromosome condensation or replication defects.

I. 6. Other Roles of Mcm10:

Mcm10 is exceptionally abundant in cells with about 40,000 molecules per haploid yeast cell **[Kawasaki *et al*., 2000]**. And studies on *Xenopus* extracts show that two molecules of Mcm10 are bound per active origin (i.e. one bound per 5000bp) **[Wohlschlegel *et al.,* 2002]**, which suggests that Mcm10 is involved in processes other than DNA replication. DNA replication, chromatin condensation and chromosome segregation are three processes that require different chromatin states: the active euchromatin and the inactive heterochromatin. DNA replication factors help regulate these different processes in the chromosome cycle and defects in their proper coordination is implicated in genomic instability that can result in cancer **[Osborn., 2002]**. Mcm10, like ORC, has been shown to interact with Drosophila heterochromatin protein 1 (HP1) an essential component of the heterochromatin complex **[Shareef et al., 2001 and Pak et al., 1997]**. Additionally, *Drosophila* tissue culture cells that were depleted in Mcm10 by RNAi could continue to proliferate despite low Mcm10 levels and this supports the idea that not all Mcm10 molecules are required for DNA replication alone [**Christensen T.W. and Tye, 2003]**. Mcm10 has been shown to be important for transcriptional gene silencing **[Apger e*t al.* 2010; Douglas N.L. *et al.,* 2005; Liachko and Tye 2005, 2009].** Studies in *S. cerevisiae* demonstrated that Mcm10 is involved in transcriptional repression of the mating-type loci **[Douglas N.L. e*t al*., 2005]**. It mediates

interactions between the silencing factor Sir2 and subunits of Mcm2-7 helicase via a ~100-residue segment at its C-terminal **Liachko and Tye, 2009]**.

In a recent study conducted by Apger *et. al*. using two Mcm10 mutant alleles namely $Mcm10^{Scim19}$ (Sensitized Chromosome Inheritance Modifier 19) and $Mcm10^{d08029}$ multiple functions of Mcm10 have also been shown in *Drosophila*. Polytene chromosome analysis of the salivary glands from the two mutant alleles exibited underreplication in $Mcm10^{d08029}$ compared to the wild type (WT) and $Mcm10^{Scim19}$ **[Apger e*t al.,* 2010]**. Visualization of the brains using ethynyl deoxyuridine (EdU) incorporation showed that the WT brains were larger than the mutant brains indicating low cell proliferation in the mutants. Additionally, the higher incorporation of EdU in the mutant brains compared to WT is indicative of an S-phase delay in the mutants. Lastly, the mitotic index data for the different combinations of the $Mcm10^{d08029}$ and $Mcm10^{Scim19}$ with the WT show fewer cells in mitosis compared to the ratios in WT. The results from this study show that *Drosophila* Mcm10 has multiple roles in S-phase as well as roles in heterochromatin formation. Analysis of the two mutant alleles indicates that the S-phase function of the C-terminal 85aa is separable from the S phase function of the rest of the protein **[Apger e*t al.,* 2010]**. And additionally, Mcm10's heterochromatic function does not require the C-terminal 85aa. It is clear from this study and other literature presented that Mcm10 is a key player in DNA replication but little is known about its involvement in the establishment of different chromatin states. In order to better understand the role of Mcm10 in establishment of different chromatin states during the endoreplication cycle of *D. melanogaster*, we examined the effects of different mutant alleles of the *D. melanogaster* Mcm10 gene on DNA replication and chromatin formation. Based on the fact that different alleles of the Mcm10 gene in *D. melanogaster* appear to have distinct effects on S phase

DNA replication and chromatin condensation we **hypothesized that "the Drosophila DNA replication factor Mcm10 has separable functions in DNA replication and chromatin dynamics."**

In order to study and characterize the role of Mcm10, in chromatin dynamics and whether these roles are separable from those in DNA replication *Drosophila melanogaster* was used as the model organism. Also commonly known as "fruit fly", *Drosophila* has been one of the most studied organisms in biological research, particularly in developmental biology and genetics. What makes *Drosophila* an ideal lab study organism is that it has a short generation (~10 – 14 days at room temperature) and has high fecundity of females. The entire genome of *Drosophila* has been sequenced since 2000 and while 50% of fly protein sequences have mammalian homologs, around 75% of known human disease genes have a recognizable match in the *Drosophila* genome. And so using a panel of Mcm10 point mutant **(Table 1)** strains I have investigated the effect of these mutants on chromosome morphology and cell cycle using larval brain tissue and effects on endoreplication using salivary glands.

Objectives of the Research

The main goal of this project was to characterize the role of Mcm10 in chromatin dynamics and DNA endoreplication.

- **Hypothesis: Drosophila DNA replication factor Mcm10 has separable functions in DNA replication and chromatin dynamics**

Objective # 1: Investigate the impact of MCM10 alleles on cell cycle and chromosome morphology

Several Mcm10 mutants in *Drosophila* were identified and/or generated in our lab and were tested for their impacts on cell cycle progression and chromosome morphology **(Table 1 & Figure 10).** 20 non-lethal homozygous mutant alleles of Mcm10 **(Table 1)** were used for this project. To investigate the role of Mcm10 in cell cycle progression mitotic index analysis was conducted in the larval brain tissue. The mitotic index data can provide information about any Synthesis phase or Mitosis phase delays. Brain squash protocol was used to look at cell proliferation in the *Drosophila* larvae. The brain has plentiful amount of cells that are undergoing a normal cell cycle progression and not endoreplication. If there are any defects in the length of time to accomplish the cell cycle, such as a delay completing the Synthesis phase or Mitosis phase, we could detect it. In addition, mitotic figures observed during the Mitotic index calculation, can be investigated to look at potential defects in

segregation and condensation of the chromosomes, providing insight into the impact of Mcm10 mutants on chromosome morphology.

<u>Objective # 2:</u> To investigate MCM10 alleles' impact on endoreplication and DNA compaction

In order to analyze the impact of these mutants on chromosome compaction, DNA content of salivary glands in the *Drosophila* nuclei was investigated and the results were compared with WT Mcm10. During the larval development in *Drosophila*, the salivary glands exhibit formation of polytene chromosomes. Polytene cells undergo multiple rounds of DNA replication, called endoreplication, producing several sister chromatids that stay synapsed without undergoing any cell division. The nuclei complete 10 successive rounds of replication by the time they are third instar larva reaching an average ploidy of 1024n **[Edgar, 2001]**. Endoreplication occurs in the salivary glands in order to produce excess glue required for pupation. Since there is no mitotic phase, the endoreplication can give information about replication defects in the S-phase. Mcm10 as discussed earlier is found to associate with chromatin in S-phase and has an essential role in replication. Hence, an analysis of the DNA compaction can give further insight into the role of Mcm10 during S-phase.

Homozygous allele	Mutation
Mcm10 [E381K]	Missense
Mcm10 [K406N]	Missense
Mcm10 [R415H]	Missense
Mcm10 [H431R]	Missense
Mcm10 [P439S]	Missense
Mcm10 [T441I]	Missense
Mcm10 [E451K]	Missense
Mcm10 [G461S]	Missense
Mcm10 [D473N]	Missense
Mcm10 [D473E]	Missense
Mcm10 [T518I]	Missense
Mcm10 [V520I]	Missense
Mcm10 [S530F]	Missense
Mcm10 [D532N]	Missense
Mcm10 [V551I]	Missense
Mcm10 [D608Y]	Missense
Mcm10 [I620F]	Missense
Mcm10 [deletion 626-628]	Deletion
Mcm10 [S629L]	Missense
Mcm10 [P692L]	Missense

Table 1. List of Mcm10 mutant alleles assayed for this study.

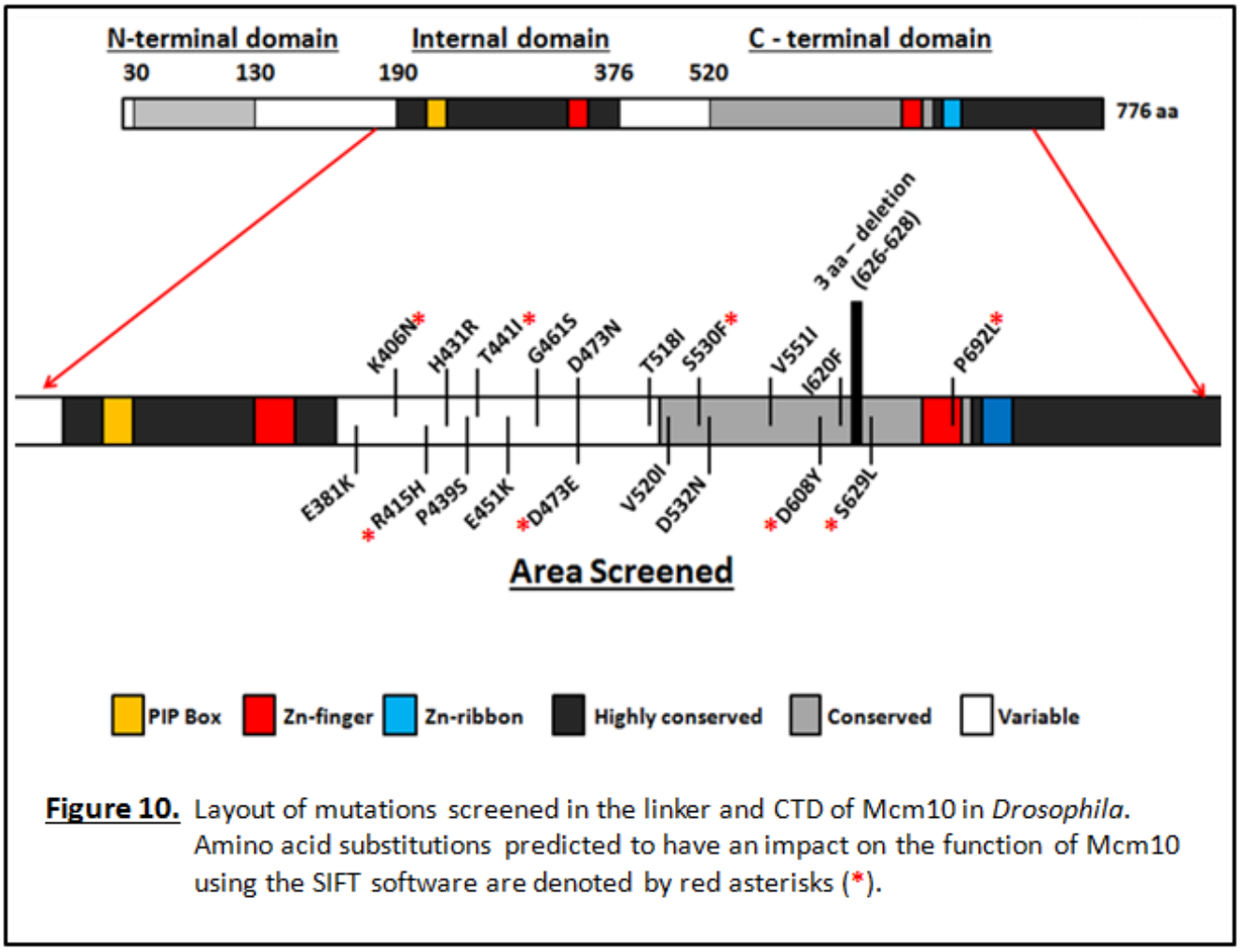

Figure 10. Layout of mutations screened in the linker and CTD of Mcm10 in *Drosophila*. Amino acid substitutions predicted to have an impact on the function of Mcm10 using the SIFT software are denoted by red asterisks (*).

Preliminary Results

Initial work on Mcm10 conducted in our lab was to look at the impact of the panel of Mcm10 point mutations on position effect variegation (PEV). Variegation effect of a euchromatic gene is caused by the inactivation of a gene in some cells through its abnormal juxtaposition with heterochromatin **[Henikoff S., 1990].** Heterochromatin represses nearby transcribable genes and this gives rise to different expression levels of the gene from cell to cell and this is demonstrated by PEV. A classic example of this is the Drosophila white mottled 4 (Wm4) mutation. Normally, the white gene is expressed in every cell of the adult *Drosophila* eye resulting in the red eye phenotype. However in the mutation, an inversion on the X-chromosome places the white gene next to the pericentric heterochromatin **[Henikoff S., 1990]**. As a result expression of the white gene gets repressed and the eye color is variegated giving a red-white mosaic color resulting in PEV. Heterochromatin protein (HP1) suppresses this PEV effect allowing the white gene to be expressed to give the red eye phenotype. PEV analysis was conducted on some of the Mcm10 mutants where the red pigment in the eyes was measured. The data collected from this analysis showed that many of the Mcm10 mutant strains (labeled in red) significantly suppressed PEV like HP1 **(Figure 11)**. This suggests that Mcm10 has a role in maintaining heterochromatin formation and different regions of Mcm10 seem to be responsible in doing so.

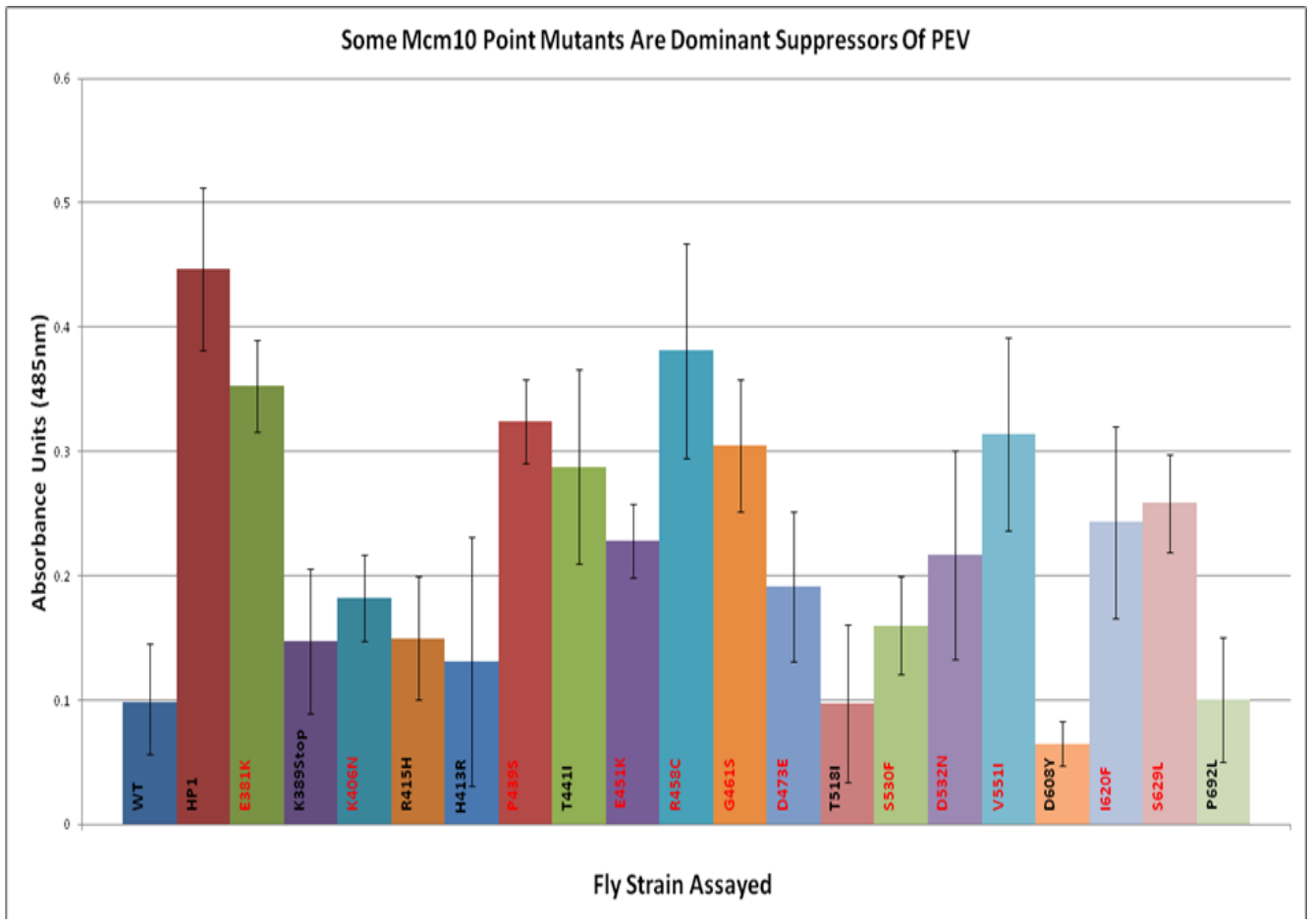

Figure 11. PEV analysis results of some Mcm10 point mutant alleles. Majority of the Mcm10 mutants are dominant suppressors of PEV. Mutants labeled in red significantly suppressed PEV like HP1 when compared to wild type.

II. MATERIALS AND METHODS

II.1 Fly husbandry/stocks:

Our lab had identified several mutant alleles for Mcm10 in *Drosophila* using literature search and tilling screens. Fly stocks with these mutant genotypes **(Table 1)** were obtained from Zucker stock center and all fly stocks were maintained on Caltech media (U.S. Biological no. D9600-07) at room temperature. Fly lines of 20 out of 30 of these alleles were homozygous viable **(Table 1)** and had been backcrossed a minimum of 8X to a balanced deficiency that spans the MCM10 region (Df(2L)/CyO, Bloomington stock#7529). **Figure 10** represents a layout of all the 20 point mutants in the CTD that were assayed in this study. These were all ethyl methanesulfonate induced mutations of which 19 were missense point mutation while 1 was a three amino acid (aa.) deletion mutation. All techniques explained below have been derived from Apger et al. (2010) and Chmielewski et al. (2011).

II.2 Prioritization of the Mcm10 Mutations

With the help of the software called SIFT (Sorting Tolerant From Intolerant) which uses sequence homology to predict whether and amino acid substitution will affect protein function and in turn alter its phenotype **[Ng P.C. and Henikoff S., 2003]**, the 20 mutations in Mcm10 gene were prioritized for the assays conducted. The software provides a score for the amino acid substitution and any score below 0.05 is considered intolerant and the substitution is predicted to affect protein function. 8 out of the 20 Mcm10 mutations used in this study had a score less than 0.05 and were predicted to have an impact of the function of Mcm10

(Figure 10, red asterisks**)**. The remaining mutations were considered tolerant changes by the software.

MCM10 alleles' impact on cell cycle and chromosome morphology

II.3. Larval Brain Squashes:

Third instar wandering larvae were harvested and brains removed, using Dumoxel^{TM} Tweezer #5, in 1% PEG 8000 in 1XPBS (140 mM NaCl, 2.7 mM KCl, 1.4 mM Na_2HPO_4, 1.8 mM KH_2PO_4) pH 7.2 solution. The brains were then transferred to a hypotonic solution (0.5% Sodium Citrate) for 10 minutes to allow the brain cells to swell. Next, the brains were transferred to a 11:11:2 Acetic acid, Methanol, Water mixture for 20 seconds to fix the cells. The brains were then transferred to a clean microscope slide and overlaid with a siliconized coverslip. The microscope slide and coverslip were sandwiched between filter paper and an additional microscope slide was then placed in machinist vise and 15 Nm of force was applied using a digital torque for 2 minutes. After removing the brains from the vice the slides were dipped in liquid nitrogen for a minute and the coverslip was removed via a razor blade. The slides were then gently washed with 100% ethanol, allowed to air dry, and were covered with 7μL of Vectashield containing DAPI (1μg/ml 4',6-diamidino-2-phenylindole). A coverslip was placed over the slide and sealed with clear Sally Hansen fingernail polish. Slides were stored at 4°C until imaging.

II.4. Microscopy for Brain Squashes:

Microscopy was performed using an Olympus IX81 Motorized Inverted Microscope with Spinning Disk Confocal. Images were analyzed using Slidebook™ software.

II.5. Mitotic Indices:

For every Mcm10 mutant strain mitotic index determination was performed on 10 larval brain squash preparations by selecting 10 random well populated fields of view for each using a 60X objective. Total mitotic figures and total number of nuclei for each field were counted using the counter tool available in Photoshop®. The number of mitotic figures were divided by the total number of nuclei in each field to generate the fraction of cells in mitosis. Statistical analysis was performed using Minitab™ Statistical Software.

II.6. Mitotic Chromosome Phenotypes' Quantitation:

Mitotic figures were counted from each of the 10 pictures from all 10 brain squash slides per mutant strain and used to calculate the mitotic index described previously. These mitotic figures were segregated into different phenotypes observed. In order to generate statistical differences, odds ratio were calculated for mitotic figures representing a phenotype versus the ones that did not present that phenotype for each category in every Mcm10 strain using JMP® Pro Statistical Discovery™ Software.

MCM10 alleles' impact on DNA Endoreplication and DNA compaction

II.7. Larval Salivary Gland Acquisition:

Wandering third instar larva were collected from age and density matched bottles and placed in a 16 well dissecting dish containing 100µl of 1x PBS. Salivary glands were isolated using Dumoxel™ #5 tweezers (Electron Microscopy Sciences, Hatfield, PA). Once salivary glands were dissected, they were transferred to a separate holding well containing 100µl 1X PBS.

II.8. Fixing tissue and DAPI Staining:

After acquiring the desired number of salivary glands, glands were transferred into a new well containing 100µl of 4% formaldehyde in 1X PBX (1x PBS with 1% Triton X-100) and allowed to incubate for 20 minutes at room temperature. After 20 minutes, the formaldehyde was carefully removed using a 200µl pipette and 100µl of fresh 1µg/ml 4',6-diamidino-2-phenylindole (DAPI) solution (diluted from 3µg/ml 100x DAPI stock with 1x PBS) was for 5 minutes in order to stain the DNA. After 5 minute incubation, the dapi solution was removed from the well and washed twice by adding 100µl in 1X PBX for 5 minutes, followed by one 45 minute wash, and one 10 minute wash at room temperature. During the final 10 minute wash, slides were prepared as discribed below:

II.9. Slide Preparation and Tissue Mounting:

Using a 20cc syringe equipped with a 22 gauge blunt fill needle filled with Vaseline®, two lines of Vaseline® were dispensed along the width of the slide (Fisherbrand® 25 x 75 x 1.0mm, Cat. No. 22-034-486) about an inch and a half apart. In the space between the two lines of Vaseline®, 30µl of Vectashield® Mounting Medium (Cat. No. H-1000, Vector Laboratories, Burlingame, CA) was dispensed along the length of the slide. When the final 10 minute wash was complete, the salivary glands were transferred to the Vectashield®. A coverslip (Fisherfinest®, 22x50-1, Cat. No. 12-548-5E) was gently placed on top of the slide being careful to avoid air bubbles. With the coverslip on the slide, the two lines of Vaseline® were tapped gently to lower the coverslip making sure the entire area between the two lines of Vaseline® had taken up by Vectashield®.

II.10. Microscopy for Salivary Glands

Microscopy was performed using the Zeiss Laser Scanning Microscope (LSM) 700 along with the Zen imaging Software.

II.11. Imaging Salivary Gland Whole Mounts:

Salivary gland nuclei are three dimensional structures and because of this, it is necessary to create a three dimensional image using the Z-stack feature of the microscope. Slides were imaged using 20X magnification. The Z-stack images were created using 10-36 2.0µm steps depending on the thickness of the salivary gland. Salivary glands are also rather large and take up multiple fields of view requiring a montage to accommodate the entire

gland in one image. Using the stitching feature of the Zen software a complete 3-D Maximum Intensity projection image of salivary gland was created. Each image was acquired using epi-fluorescence with a DAPI filter. Images were saved as .czi files which were then exported as .tiff files for analysis using Adobe® Photoshop® elements CS4.

II.12. Salivary Gland Nuclei Size Analysis:

The first step to determining salivary gland nuclei volume was to set the appropriate parameters in Photoshop®. To account for the difference in pixel length between Slidebook™ and Photoshop®, the measurement scale in Photoshop® was adjusted. In the measurement scale setting pixel length was set to 1 and the logical length will be set to 1.595. The wand tool was used to select individual salivary gland nuclei. With the parameters set, individual nuclei in a gland were selected and the measurements were recorded. These measurements were exported as .txt files and transferred into Excel® spreadsheets.

II.13. Determining Average Volume of Salivary Gland Nuclei:

Statistical analysis was performed using Minitab® 14 Statistical Software. The area of each salivary gland pair nuclei was averaged and data was recorded in an Excel® sheet. The mean, standard deviation, and standard error of the data was calculated and used to determine DNA volumes. Using the area of a circle equation($A = \pi r^2$) the area of each data point was converted into a radius. Next, using the volume of a sphere formula ($v = \frac{4}{3}\pi r^3$) values for each radius were converted into volumes. Volume measurements were then transferred into Minitab® to get statistical analysis data.

II.14. Salivary Gland Nuclei Counts:

Using the counter tool available in Photoshop®, nuclei counts were taken from ten individual salivary glands. The total number of nuclei for each gland pair were then averaged and recorded in Excel®.

II.15. Salivary Gland Digestion and DNA Extraction:

The salivary glands of third instar wandering larva were dissected in 150µl of HyQ® Graces's Unsupplemented Insect Cell Culture Medium (Cat No. 30610.01, HyClone, Logan, UT) and transferred to a holding well also containing 150µl of Grace's. Once the desired number of salivary glands were acquired in the holding well, glands were transferred to PCR tubes (Fisherbrand®, Cat. No. 14230225) prefilled with 3-5x 1mm glass beads (BioSpec Products, Inc., Cat. No. 11079110) along with 300 micron glass beads (Sigma®, 212-300microns Unwashed, Lot. No. 033K1546) and 25µl of squishing buffer (20µg/ml proteinase K, 10mM Tris-base, 25mM NaCl, and 1mM EDTA). Each tube received one pair of glands. PCR tubes were then vortexed at max speed for 15 seconds and centrifuged to collect liquids. PCR tubes were then placed in a thermocycler (C1000™ Thermo Cycler, Biorad®) and incubated at 37°C for 30 minutes then heated to 85°C for 10 minutes. After incubation, the PCR tubes were vortexed for 15 seconds and centrifuged at 12,000 rpm for 2 minutes.

Note: At this point extracts were frozen at -20°C until desired number of digestions had been completed.

II.16. Salivary Gland DNA Quantitation:

DNA content values were determined using the Qubit® dsDNA HS Kit (Qubit® dsDNA HS Assay Kit, Invitrogen™, Cat. No. Q32854) along with the Qubit 2.0 Fluorometer™ (Invitrogen™, Cat. No. Q32866). The Qubit® dsDNA HS Kit consists of a highly sensitive dye that is specific to dsDNA over RNA and common contaminants, such as salts, free nucleotides, solvents, detergents, or protein are well tolerated in the assay. The Qubit® working solution was prepared by diluting the Qubit® reagent 1:200 in Qubit® buffer. 190µl of Qubit® working solution was transferred to Qubit® assay tubes (Invitrogen™, Cat. No. Q32856) along with 10µl of salivary gland DNA extract. After Qubit® working solution and salivary gland DNA extract were loaded, each tube was gently vortexed to mix and spun for 10 seconds to collect liquid at the bottom of each tube. DNA content values were determined using the Qubit® 2.0 Fluorometer. The Qubit® 2.0 Fluorometer was standardized using two standard solutions provided in the Quant-iT™ dsDNA HS Kit.

III. RESULTS

III.1. Mitotic Index Analysis:

3rd instar brain nuclei and mitotic figures from a collection of the 20 *D. melanogaster* Mcm10 gene mutant strains were analyzed. **Figure 12** shows images of brain squashes from WT and a couple of Mcm10 mutant strains, namely, K406N and E451K. The images were pseudo-colored from blue to green for better visualization. Mitotic indices for all the strains were calculated based on the number of mitotic figures observed with respect to the total number of mitotic and non-mitotic nuclei. An average mitotic index value was generated per brain and the ten averages for each strain were converted into box plots **(Figure 13).** The results show that none of the Mcm10 mutant strains had significantly different fraction of cells in mitosis than in the WT as the p-values were all greater than 0.05.

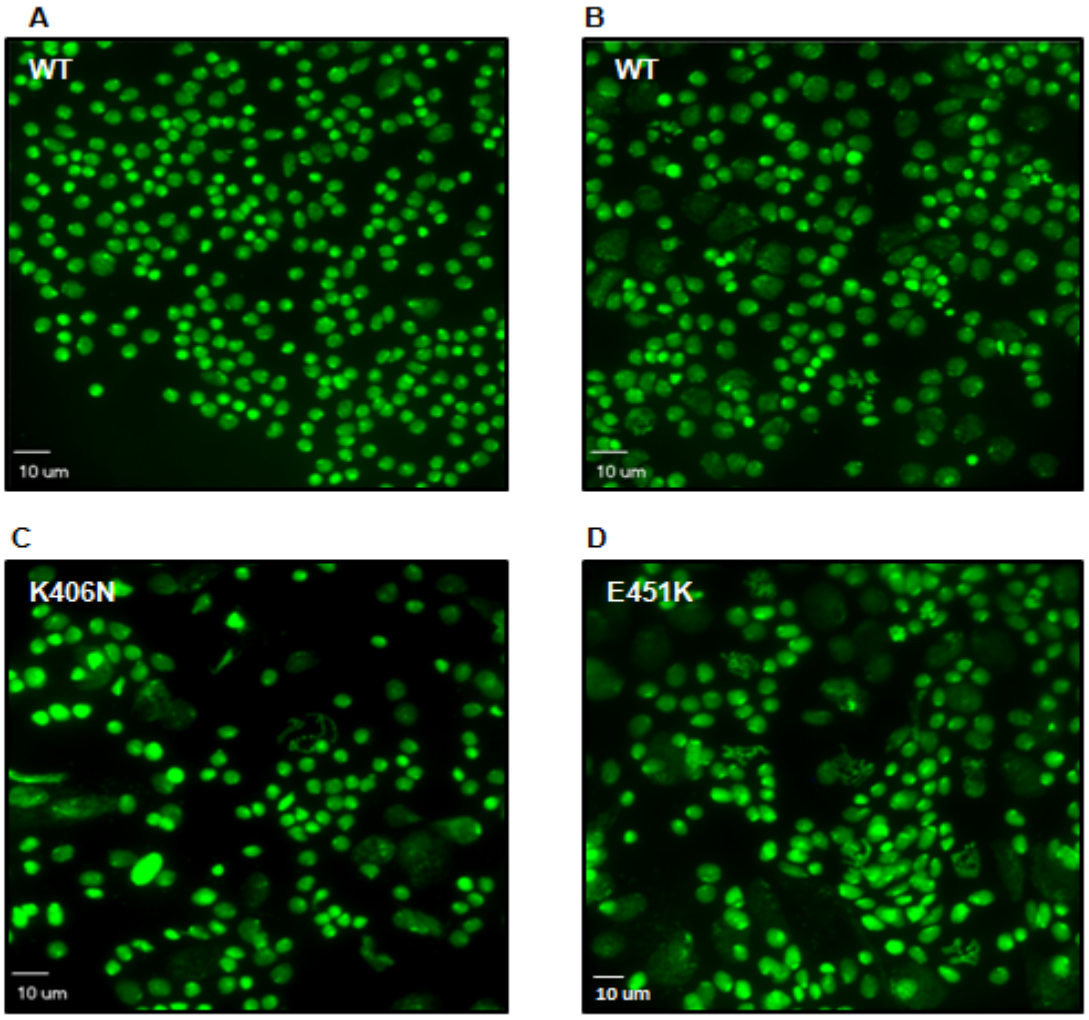

Figure 12. Brain squash images from WT Mcm10 **(A,B)** and Mcm10 mutant strains K406N **(C),** and E451K **(D).**

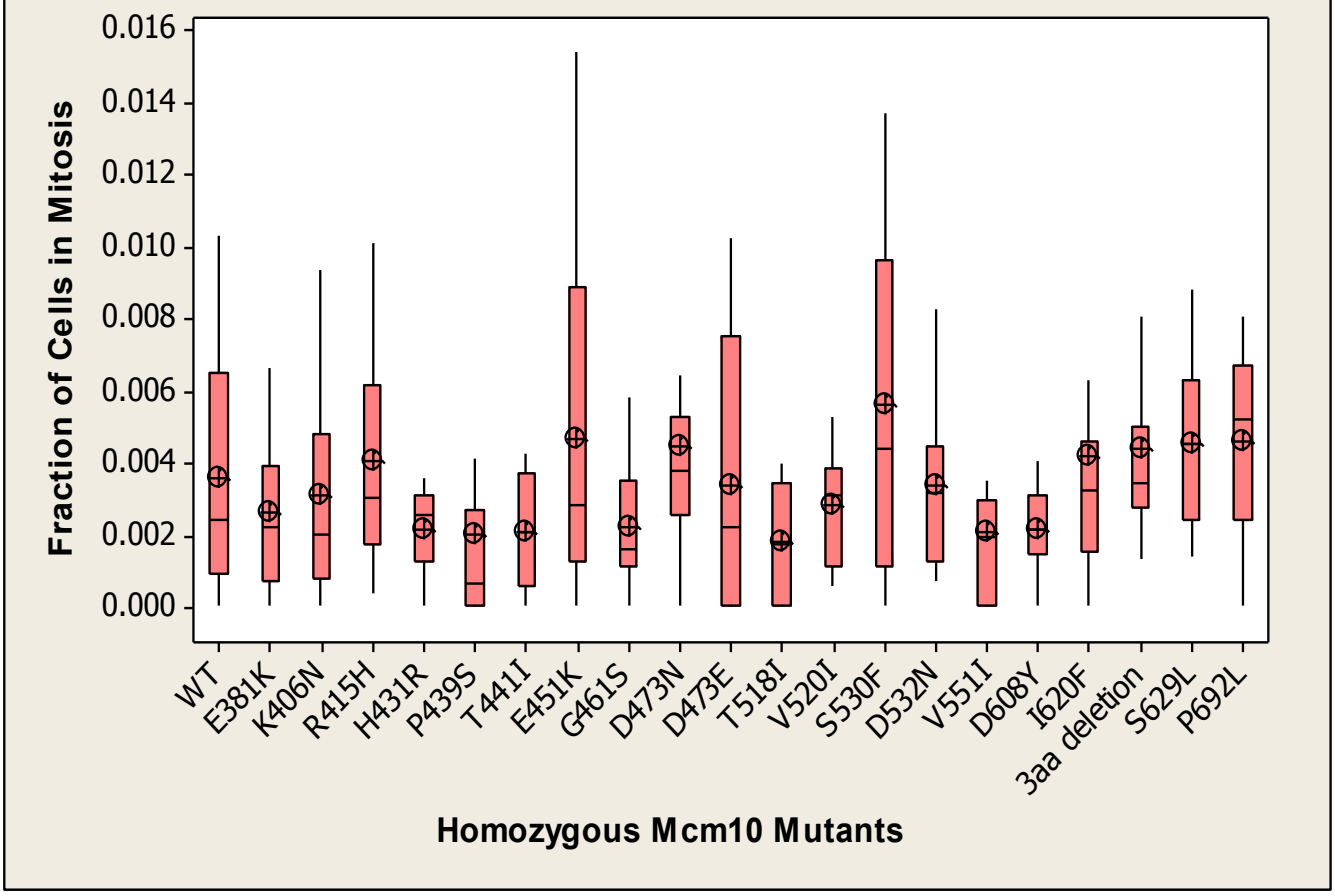

Figure 13. Mitotic index analysis of the homozygous Mcm10 mutant alleles and their comparison to wild type (WT) Mcm10. Box plots of the fraction of cells in mitosis were generated using the Minitab® software and statistical analysis using students paired t-test. The results show that there was no significant delay in the progression of cell cycle through M-phase in any of the Mcm10 mutant strains when compared to WT (p values > 0.05). ⊕ represents the mean value.

III.2. Phenotypes Associated with Mitotic Figures:

In addition to conducting the mitotic index analysis we also examined the phenotypes of the mitotic figures seen in all the 100 pictures taken per strain (10 images of 10 individual brain squashes). The normal mitotic figure of a somatic cell in *Drosophila* should consist of four pairs of chromosomes as shown in **Figure 14A**. Although the Mcm10 mutant strains showed no significant delay in progression through the M-phase, several different mitotic figure defects were observed in the chromosomes. These include phenotypes such as separated sister chromatids **(Figure 14B)**, chromosome condensation defects **(Figure 14C)**, chromosome breaks **(Figure 14D),** anaphase bridge defects **(Figure 14E)**, and aneuploidy **(Figure 14F)**.

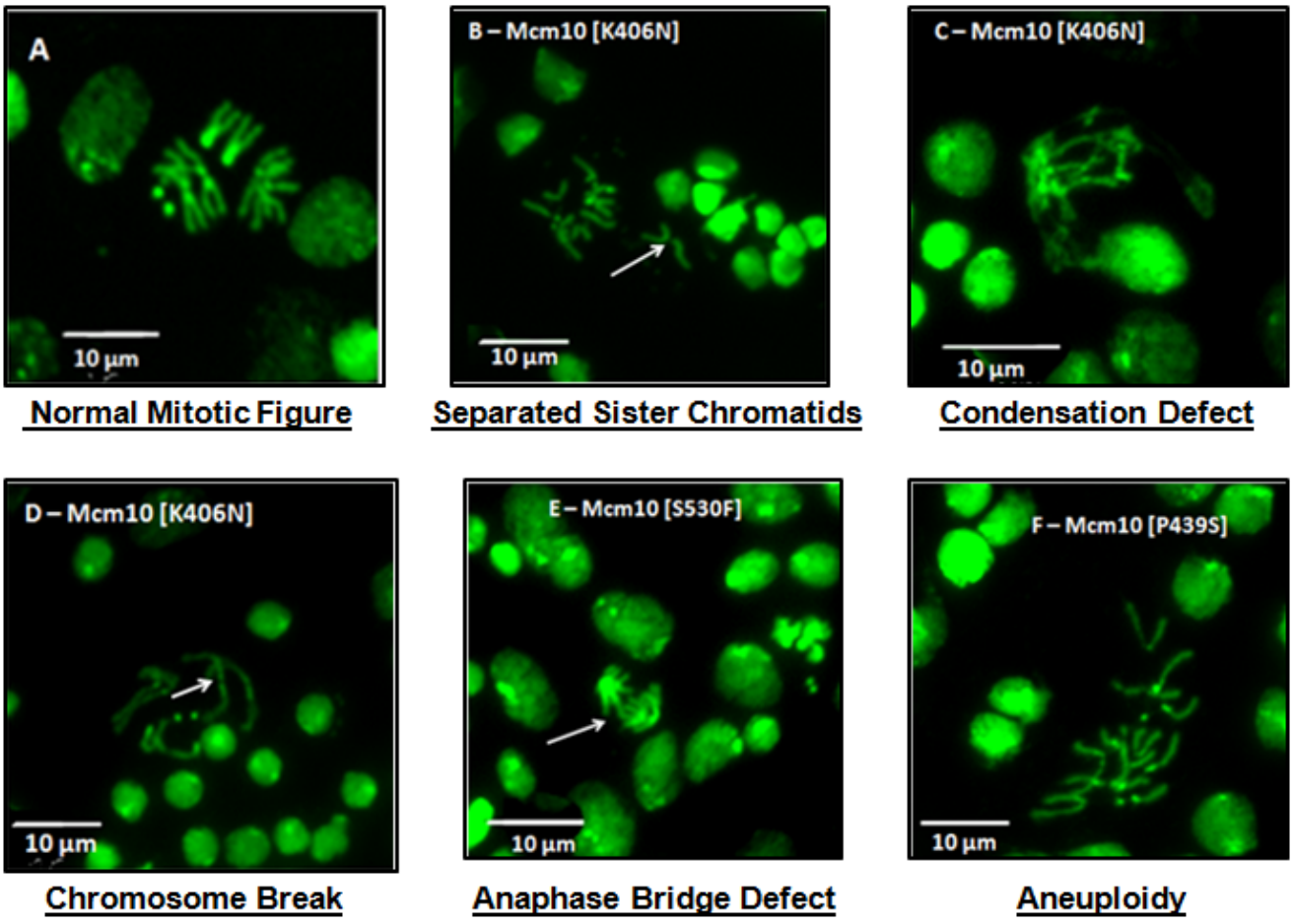

Figure 14. Mitotic chromosome phenotypes associated with Mcm10 mutants. **(A)** Normal mitotic figure in a somatic cell of *Drosophila* consists of four pairs (2n) of chromosomes. **(B-F)** Mitotic figures observed in the brain squash images (used for mitotic index calculations) of the Mcm10 mutants show a range of chromosome defects such as separated sister chromatids, severe condensation defect, chromosome breaks, defects in anaphase bridge, and aneuploidy.

III.3. Quantitation of the Mitotic Chromosome Phenotypes:

Aberrant mitotic figures were observed in each of the Mcm10 mutant strains but in varying types and levels. And so to further investigate this phenomenon all the mitotic figures were sorted, from each of the images used to calculate the mitotic index, into the different defects and their percentages were calculated. Bar graphs were generated to represents the percentage of normal and defective mitotic figures **(Figure 15)**. Additionally, odds ratios test was conducted on all phenotypes using the JMP® Pro Statistical Discovery™ Software which generated p-values comparing the WT and mutant strains. However, due to the nature of the data collected and limitation of statistical tests that could be done, any data with "zero" value failed to generate statistical values **(Table 2)**. For this reason, since the WT had a zero value for aneuploidy, we were unable to compare the aneuploidy results from mutant strains and WT in order to get statistical p-values.

The total number of mitotic figures counted in the different Mcm10 strains ranged from 30 – 90 figures. The mitotic figures were grouped into six chromosome phenotypes and their percentages per strain were calculated and arranged to generate a bar graph **(Figure 15).** These results show that all Mcm10 mutants display significant amounts of defective mitotic chromosomes. Only values greater than 5% have been displayed on the graph. WT Mcm10 had about 82% normal mitotic figures while all other mutants (except E381K, $p = 0.0552$) showed significantly lower levels of normal mitotic chromosomes (blue bars, **Figure 15** and p values > 0.05, **Table 2**). The most common aberrant phenotype observed was a defect in condensation of the chromosomes **(Figure 14C)**. However, the severity of condensation defect varied as the mutant strains displayed a range of 19% to 63% (red bar,

Figure 15) when compared to wild type. Strains E451K, D473E, V520I, S530F and D532N do not show significant condensation defects compared to the 10% observed in WT (p-values > 0.05, **Table 2).** However, all other mutants displayed high levels of condensation defect ranging from 25% to 63% (p-values $\leq$ 0.05, **Table 2**). It is important to note here that if the chromatin was not organized into chromosomes as seen in **figure 14A**, then the defect was characterized as condensation defect **(Figure 14C)**.

It is interesting to see that apart from condensation defects, different mutations in Mcm10 led to different levels of other chromosome aberration such as aneuploidy, anaphase bridge defects, and separated sister chromatids. For instance, P439S and D532N show highest percentage of aneuploidy (10%, and 24%, respectively), while strains V551I and P692L along with the wild type display no aneuploidy. Many of the mutant strains showed a slightly higher defect in anaphase bridges as well (purple bar, **Figure 15**) compared to other phenotypes. Only strains E451K and P692L show about 12% anaphase bridge defect which is significantly higher when compared to WT (p-values = 0.0318 and 0.0450, respectively). Likewise, a significant proportion of separated sister chromatids was observed only in strain I620F (11.4%, p-value = 0.0450). The top most bars in **Figure 15** represent “other” defects which were phenotypes that were difficult to assign to existing categories because either the chromosomes itself were severely defective beyond recognition or it was hard to distinguish the mitotic figures due to the nature of resolution of the images. However, in addition to all the phenotypes observed, mutant K406N also showed chromosome with broken arm **(Figure 14D)** and this was grouped within the “other” defects since chromosome breaks were not observed in any of the other Mcm10 strains. These results suggest that the Mcm10 mutants

examined progress through M-phase comparable to WT. However, they are more prone to defects in chromatin condensation and chromosome segregation than in WT.

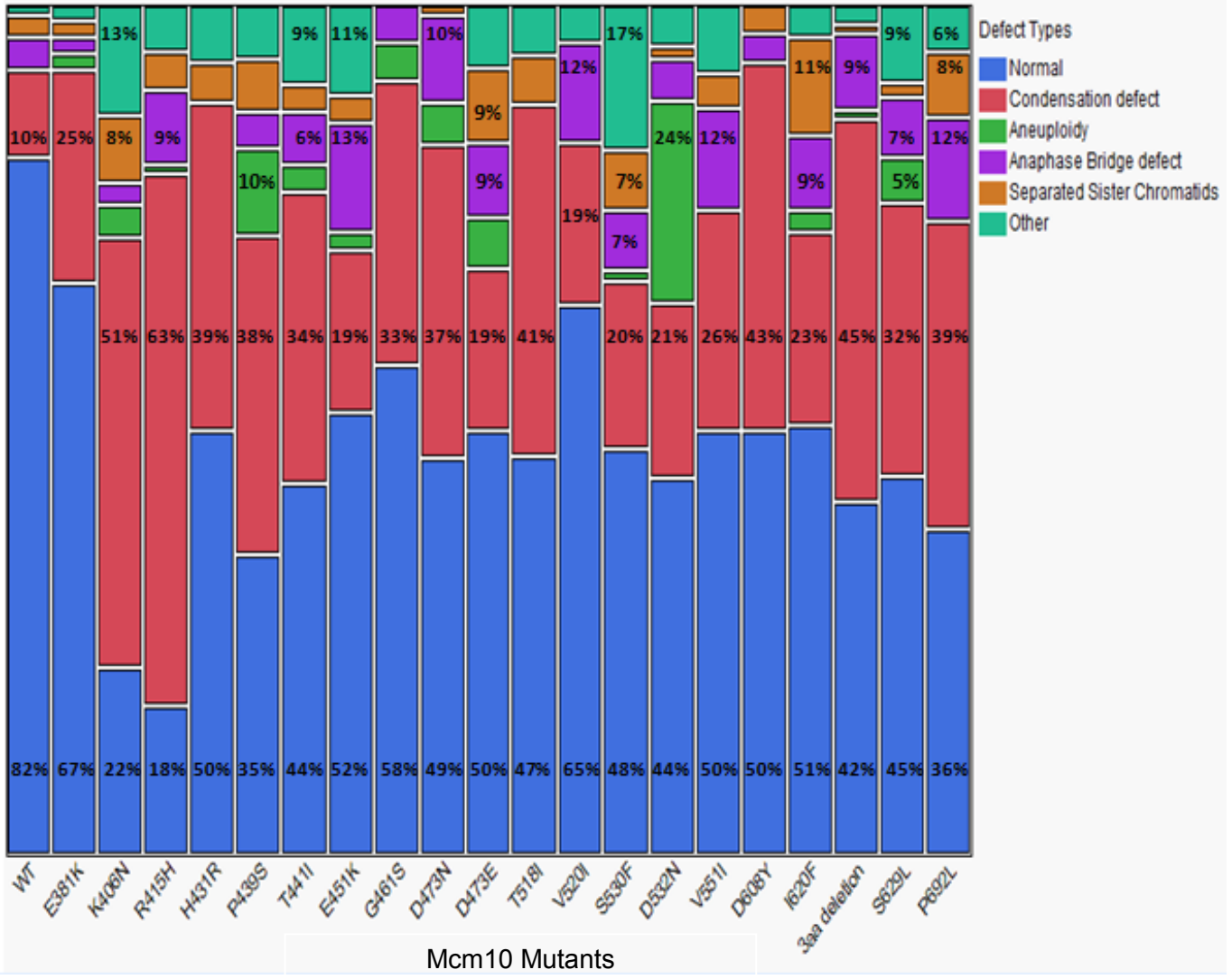

Figure 15. Bar graph representing the percentages of normal and defective mitotic chromosome phenotypes. Values less than 5% are not shown.

Mcm10 Strain	Normal	Condensation Defect	Aeuploidy	Anaphase Bridge Defect	Separated Sister Chromatids	Other Defects
WT	82.1%	10.3%	0%	3.85%	2.56%	1.28%
E381K	67.3% (p = 0.0552)	25% (p = 0.0268)*	1.92%	1.92% (p=0.5216)	1.92% (p = 0.8095)	1.92% (p = 0.7733)
K406N	22.1% (p < 0.0001)*	50.5% (p < 0.0001)*	3.9%	2.6% (p=0.6587)	7.8% (p = 0.1330)	13% (p = 0.0024)*
R415H	17.6% (p < 0.0001)*	62.6% (p < 0.0001)*	1.09%	8.79% (p = 0.1843)	4.4% (p = 0.5162)	5.5% (p = 0.1208)
H431R	50% (p = 0.0002)*	38.6% (p = 0.0002)*	0%	0%	4.55% (p = 0.5628)	6.82% (p = 0.1065)
P439S	35.4% (p < 0.0001)*	37.5% (p = 0.0001)*	10.4%	4.25 (p = 0.8722)	6.3% (p =0.2783)	6.3% (p = 0.1097)
T441I	43.8% (p < 0.0001)*	34.4% (p =0.0093)*	3.1%	6.3% (p =0.5931)	3.1% (p = 0.8714)	9.4% (p = 0.0398)*
E451K	52.1% (p < 0.0001)*	19.2% (p = 0.0991)	2.1%	12.8% (p = 0.0318)*	3.2% (p = 0.8066)	10.6% (p = 0.0067)*
G461S	57.8% (p = 0.0038)*	33.3% (p = 0.0019)*	4.44%	4.44% (p = 0.8722)	0%	0%
D473N	46.8% (p < 0.0001)*	36.7% (p < 0.0001)*	5.06%	10.1% (p = 0.1166)	1.27% (p = 0.5483)	0%
D473E	50% (p < 0.0001)*	19.1% (p = 0.4835)	5.88%	8.82% (0.2102)	8.82% (p = 0.0925)	7.35% (p = 0.0555)
T518I	47.1% (p = 0.0002)*	41.2% (p = 0.0003)*	0%	0%	5.88% (p = 0.4034)	5.88% (p = 0.1890)
V520I	64.7% (p =0.0059)*	19.1% (p = 0.1028)	0%	11.8% (p = 0.0795)	0%	4.41% (p = 0.2585)
S530F	47.9% (p < 0.0001)*	19.7% (p = 0.1028)	1.4%	7.1% (p = 0.3861)	7.1% (p = 0.1918)	17% (p = 0.0003)*
D532N	44.4% (p < 0.0001)*	20.6% (p = 0.0858)	23.8%	4.8% (p = 0.7894)	1.6% (p = 0.6857)	4.8% (p = 0.2062)
V551I	50% (p = 0.0001)*	26% (p = 0.0204)*	0%	12% (p = 0.0825)	4% (p = 0.6526)	8% (p = 0.0556)
D608Y	50% (p =0.0011)*	43.3% (p =0.0002)*	0%	3.33% (p = 0.8984)	3.33% (p = 0.8306)	0%
I620F	50.6% (p < 0.0001)*	22.7% (p = 0.0327)*	2.5%	8.9% (p = 0.1922)	11.4% (p = 0.0245)*	3.8% (p = 0.3063)
3aa. Del. (626-228)	41.6% (p < 0.0001)*	44.9% (p < 0.0001)*	1.12%	8.99% (p = 0.1722)	1.12% (p = 0.4823)	2.25% (p = 0.6354)
S629L	44.6% (p < 0.0001)*	32.1% (p = 0.0016)*	5.4%	7.1% (p = 0.4016)	1.8% (p = 0.7611)	9% (p = 0.0320)*
P692L	38.5% (p < 0.0001)*	36.3% (p < 0.0001)*	0%	12.1% (p = 0.0450)*	7.69% (p = 0.1260)	5.49% (p = 0.1208)

Table 2. Number of mitotic figures converted into percentages within each strains and likelihood odds ratio tests conducted using actual count of mitotic figures in respective phenotypes. P-values are representative of phenotype comparisons of Mcm10 mutant strains to WT and were generated using the JMP Pro Statistical Software. All significant p-values ($p \leq 0.05$) are shown in red and denoted with a *. The software was unable to generate any statistical values for data that had zero mitotic figures in the respective field. Hence no p-values are provided for aneuploidy since WT had 0%.

III.4. Endoreplicaton:

In order to analyze the impact of the Mcm10 mutants on endoreplication, DNA compaction analyses were conducted on 18 out of the 20 Mcm10 mutants using whole mount images and the DNA content measurements of the salivary glands. Whole mount images of salivary glands from WT, H431R, E381K and I620F are shown in **figure 16**. Five salivary gland whole mounts were conducted from each Mcm10 strain, and differences were observed in the volume and the number of nuclei of these glands. Strain E381K showed abnormal distribution of the nuclei throughout the gland **(Figure 16C)** compared to the normal even spacing of nuclei observed in WT **(Figure 16A)**. This kind of uneven spacing of nuclei was also observed in some glands of strains H431R, T518I, V520I, and S530F (pictures not shown). As shown in **figure 16** the number and volume of nuclei in E381K also seemed less than in WT. In order to make sense of these differences observed qualitatively, it was necessary to determine these differences quantitatively as well. Hence, the average packaging ratios for the DNA content per unit volume in the nuclei was calculated using a novel method as described in the method and material **[Chmielewski J.F. and Christensen T.W. 2011]**. Average values of the different components of the DNA compaction analysis conducted on the Mcm10 strains have been shown in table 3. Paired t-test comparisons were conducted on the volume of nuclei, number of nuclei and the DNA content in the gland pair for each WT and Mcm10 mutant pair and the p-values are shown in **table 4**.

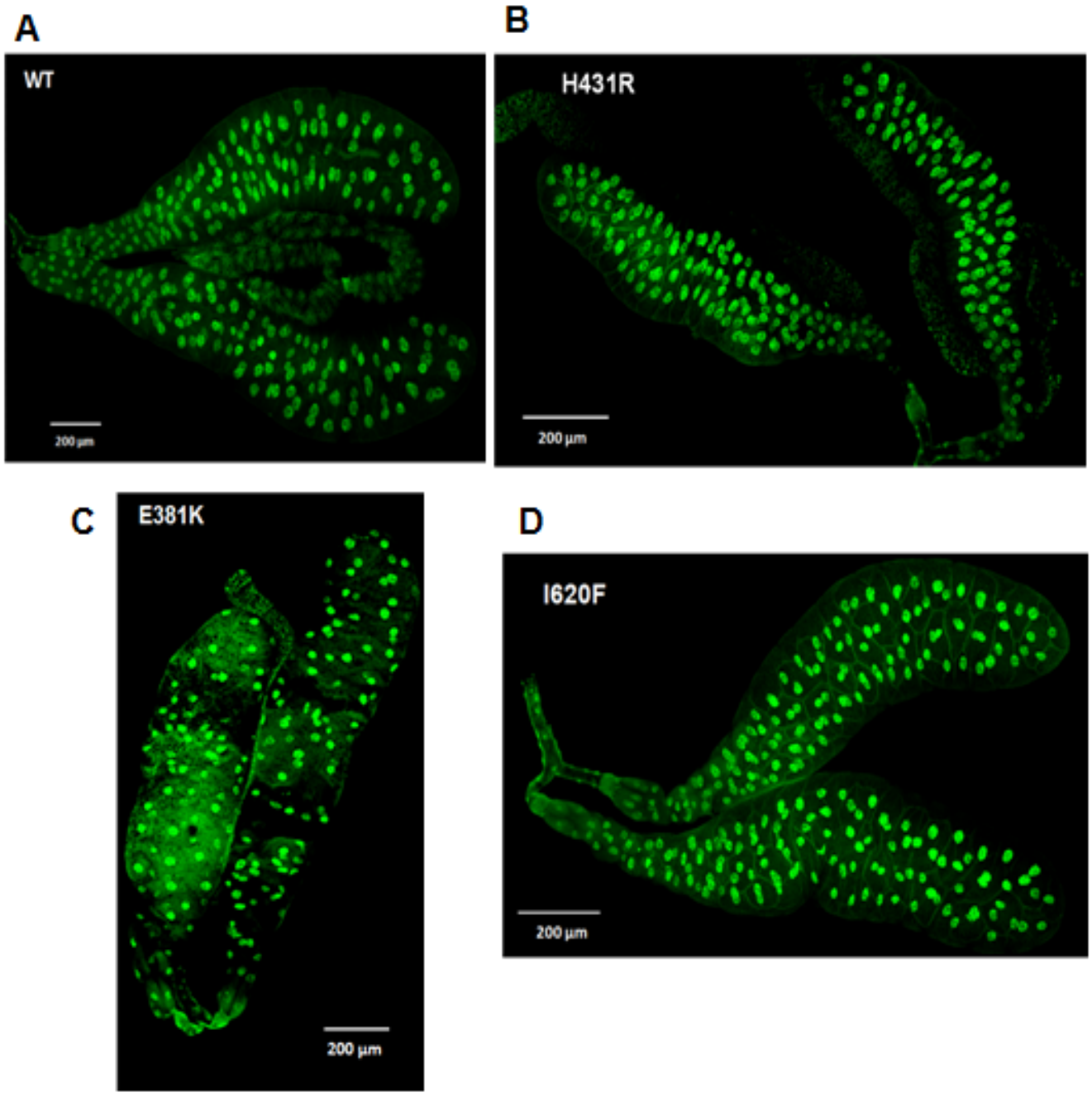

Figure 16. Salivary gland images from WT **(A),** and Mcm10 mutant strains [H431R] **(B)**, [E381K] **(C)** and [I620F] **(D).**

Table 3. A

	Genotype						
	WT	E381K	K406N	R415H	H431R	P439S	T441I
Volume of Nuclei (μm^3)	39286 ± 4002	24119 ± 2836	84684 ± 5975	29328 ± 4192	23222 ± 2647	67032 ± 16205	45870 ± 4473
# of Nuclei per Gland Pair	247.2 ± 16.38	178.8 ± 7.03	98.4 ± 7.54	184.4 ± 38.68	176.6 ± 7.00	227.4 ± 14.62	248.6 ± 19.96
DNA Content (ng / gland pair)	359.48 ± 51.83	494.24 ± 43.12	649.44 ± 67.2	541.8 ± 53.54	399.68 ± 24.07	471.8 ± 45.98	1645 ± 150.04
DNA/ Nuclei (pg)	1454.21	2764.21	6600	2938.18	2263.19	2074.76	6619.15
Packing ratio (pg / μm^3)	0.0370	0.1146	0.0779	0.1002	0.0975	0.0310	0.1443

Table 3. B

	Genotype						
	WT	E451K	G461S	D473E	T518I	V520I	S530F
Volume of Nuclei (μm^3)	39286 ± 4002	23996 ± 975	42252 ± 4797	48599 ± 6244	30470 ± 4799	27874 ± 3723	25532 ± 4467
# of Nuclei per Gland Pair	247.2 ± 16.38	207.8 ± 8.42	193.8 ± 27.15	148 ± 19.33	184.2 ± 10.97	159.8 ± 10.07	135.2 ± 21.10
DNA Content (ng / gland pair)	359.48 ± 51.83	272.92 ± 47.36	404.4 ± 57.68	1384.08 ± 124.23	346 ± 29.13	550.12 ± 42.02	426.68 ± 36.7
DNA/ Nuclei (pg)	1454.21	1313.38	2086.69	9351.89	1878.39	3442.55	3155.92
Packing ratio (pg / μm^3)	0.0370	0.0547	0.0494	0.1924	0.0616	0.1235	0.1236

Table 3. C

	Genotype						
	WT	D532N	V551I	D608Y	I620F	Del. (626-628)	P692L
Volume of Nuclei (μm^3)	39286 ± 4002	24777 ± 3517	29994 ± 6405	24883 ±3919	18388 ± 1527	43543 ± 7934	22571 ± 889
# of Nuclei per Gland Pair	247.2 ± 16.38	137.2 ± 16.74	206.4 ± 24.48	209.6 ± 10.11	219.8 ± 5.16	199.8 ± 4.11	213.8 ± 8.67
DNA Content (ng / gland pair)	359.5 ± 51.83	620.1 ± 49.43	426.44 ± 46.4	472.96 ± 33.31	361.52 ± 30.44	1294 ± 145.39	421.86 ± 86.66
DNA/ Nuclei (pg)	1454.21	4519.53	2066.09	2256.49	1644.77	6476.32	1973.13
Packing ratio (pg / μm^3)	0.0370	0.1824	0.0689	0.0907	0.0894	0.1487	0.0874

Table 3. Average values ± standard error of the different components of the DNA compaction analyses.

Table 4

Mcm10 Mutant / Relative to WT	Fold Relative to WT: Volume of Nuclei (μm^3)	# of Nuclei per Gland Pair	DNA Content (ng / gland pair)	DNA (pg) / Nuclei	Packing Ratio (pg / μm^3)
E381K	0.61 (p = 0.064)	0.72 (p = 0.029)*	1.38 (p = 0.024)*	1.90	3.10
K406N	2.16 (p = 0.005)*	0.40 (p = 0.002)*	1.81 (p = 0.003)*	4.54	2.11
R415H	0.75 (p = 0.148)	0.75 (p = 0.187)	1.51 (p = 0.027)*	2.02	2.71
H431R	0.59 (p = 0.033)*	0.92 (p = 0.018)*	1.11 (p = 0.484)	1.56	2.63
P439S	1.71 (p = 0.230)	0.92 (p = 0.448)	1.31 (p = 0.127)	1.43	0.84
T441I	1.17 (p = 0.110)	1.01 (p = 0.962)	4.58 (p < 0.000)*	4.55	3.90
E451K	0.61 (p = 0.026)*	0.84 (p = 0.118)	0.76 (p = 0.261)	0.90	1.48
G461S	1.08 (p = 0.692)	0.78 (p = 0.076)	1.12 (p = 0.585)	1.44	1.33
D473E	1.24 (p = 0.086)	0.60 (p = 0.024)*	3.85 (p < 0.000)*	6.43	5.20
T518I	0.78 (p = 0.217)	0.75 (p = 0.060)	0.96 (p = 0.810)	1.29	1.67
V520I	0.71 (p = 0.035)*	0.65 (p = 0.021)*	1.53 (p = 0.017)*	2.37	3.33
S530F	0.65 (p = 0.158)	0.55 (p = 0.004)*	1.19 (p = 0.248)	2.17	3.33
D532N	0.63 (p = 0.075)	0.56 (p = 0.001)*	1.73 (p = 0.001)*	3.11	4.93
V551I	0.76 (p = 0.396)	0.84 (p = 0.252)	1.19 (p = 0.257)	1.42	1.86
D608Y	0.63 (p = 0.107)	0.85 (p = 0.123)	1.32 (p = 0.067)	1.55	2.45
I620F	0.47 (p = 0.005)*	0.89 (p = 0.236)	1.01 (p = 0.975)	1.13	2.41
3aa. Del. (626-628)	1.11 (p = 0.573)	0.81 (p = 0.079)	3.60 (p < 0.000)*	4.45	4.02
P692L	0.57 (p = 0.025)*	0.87 (p = 0.195)	1.18 (p = 0.576)	1.36	2.36

Table 4. Fold values of genotypes' averages relative to wild type averages. Paired t-test performed to generate p-values using Minitab® software. Significant differences are represented in red ($p \leq 0.05$)*.

Using images of the 5 salivary gland whole mounts the volume of nuclei was calculated as discussed in the materials and methods section and an average volume per gland pair ± standard error is reported in table 3. Next the average values from the each mutant strain were divided by the average volume from WT which gave a fold number relative to WT shown in **table 4** and **figure 17A**. The fold values relative to WT are presented as bar graphs in **figure 17A** where "1" represents WT value. All significantly different volumes are represented by dark blue bars with asterisks in **figure 17A** and the location of the mutations are highlighted in red **(Figure 17B)**. This graph along with values from **table 4** shows that the volume of nuclei in the Mcm10 mutant strains varied compared to WT such that majority of the nuclei volumes were lower compared to WT. Strain K406N showed significantly greater volume of nuclei, over 2 fold compared to WT while other strains like H431R, E451K, V520I and P692L showed significantly lower volume of nuclei compared to WT.

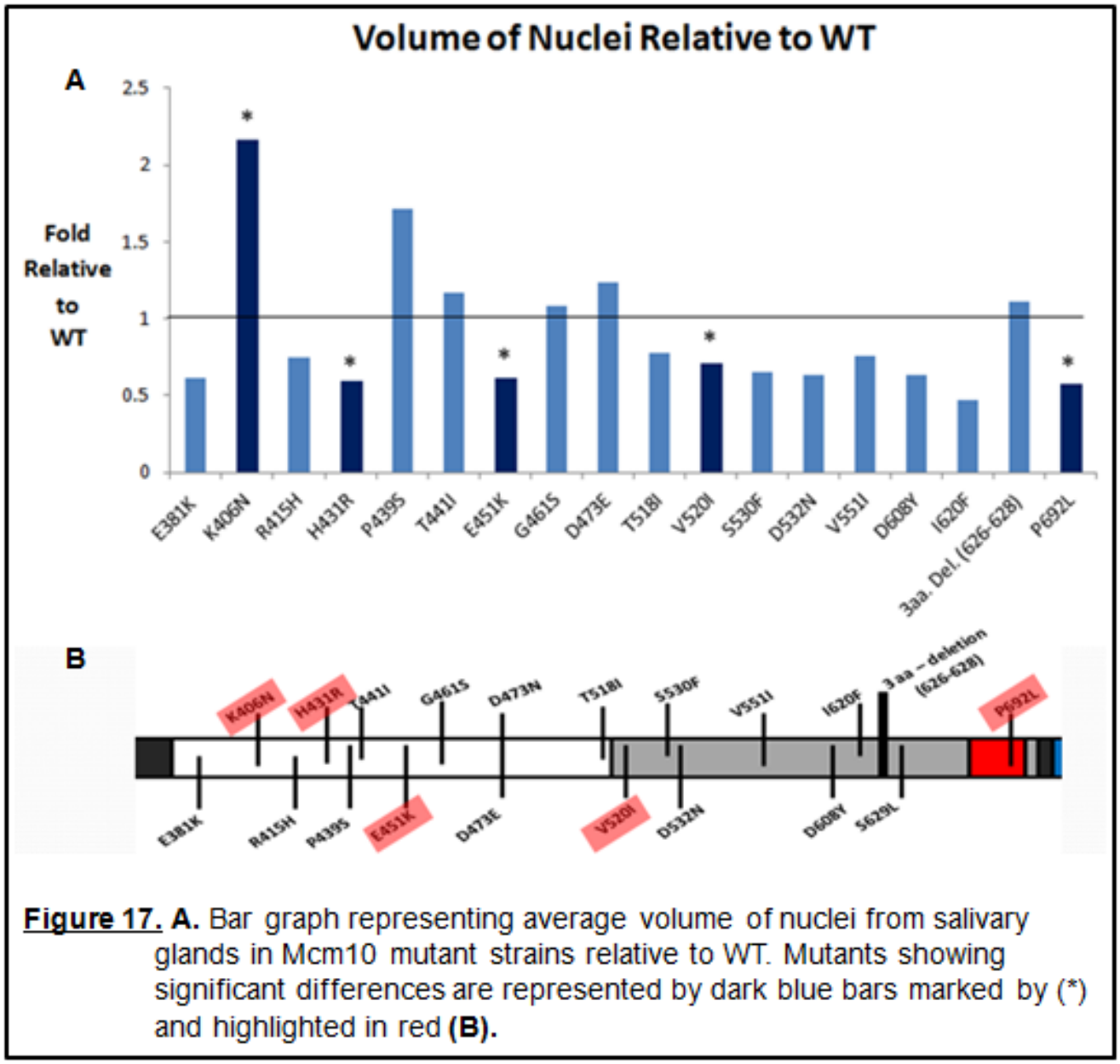

Figure 17. A. Bar graph representing average volume of nuclei from salivary glands in Mcm10 mutant strains relative to WT. Mutants showing significant differences are represented by dark blue bars marked by (*) and highlighted in red **(B).**

Next the number of nuclei was counted in each of the salivary gland using the 5 whole mount images. As discussed above the average values from Mcm10 mutant strains relative to WT were generated **(table 4)** and the data is represented as bar graphs in **figure 18A**. These results showed that the salivary glands from all Mcm10 mutant strains (except T441I)

had lower number of nuclei when compared to WT. Of these, strains E381K, K406N, H431R, D473E, V520I, S530F and D532N showed significantly lower number of nuclei compared to WT **(Table 4 & Figure 18)**. Additionally, strains K406N, H431R and V520I also showed a significantly different volume of the nuclei compared to WT.

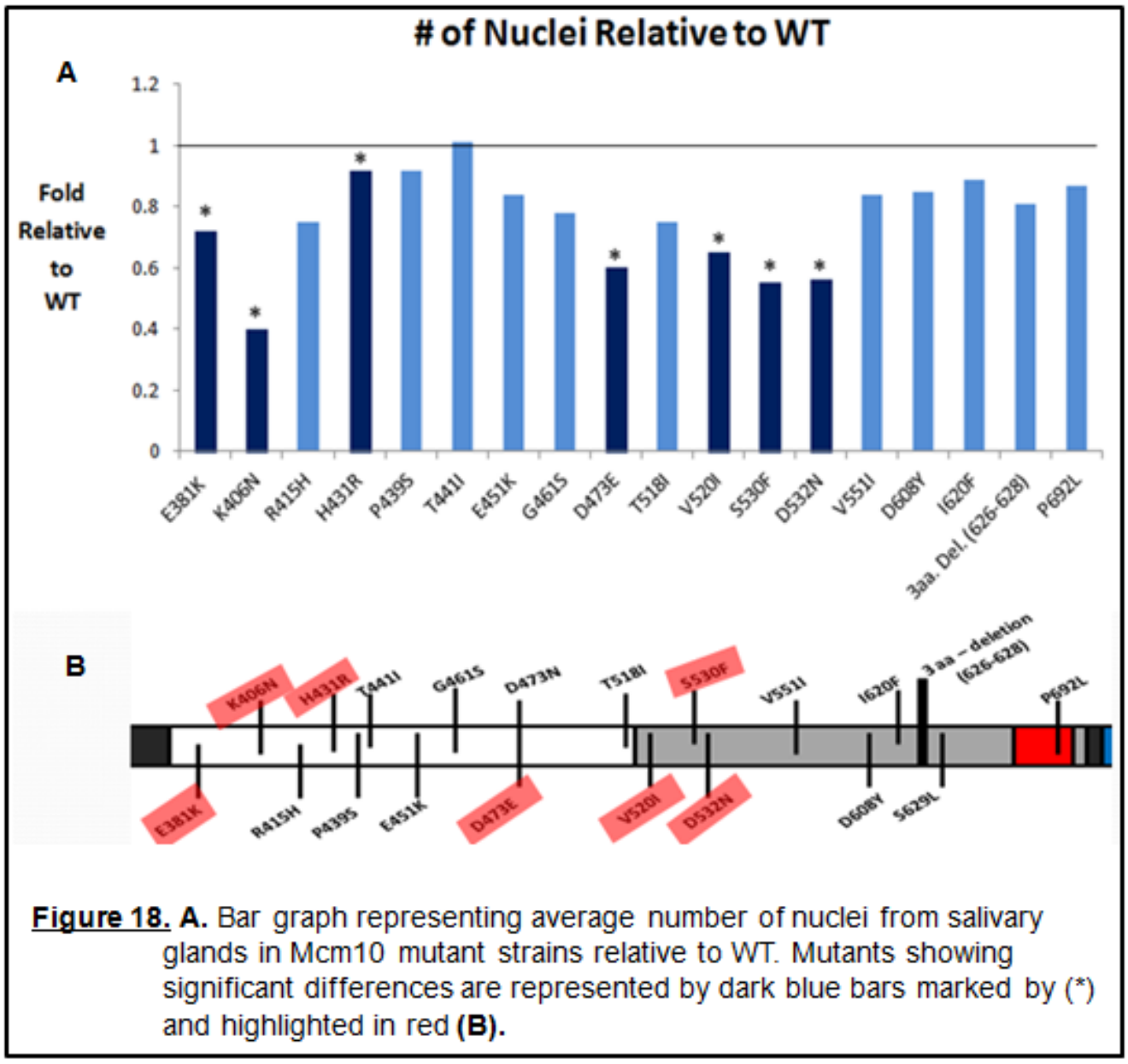

Figure 18. A. Bar graph representing average number of nuclei from salivary glands in Mcm10 mutant strains relative to WT. Mutants showing significant differences are represented by dark blue bars marked by (*) and highlighted in red **(B).**

After calculating the volume and the number of nuclei from the salivary glands, next the average DNA content per nuclei was calculated using the DNA content measured from the 25 pairs of salivary glands and the values were each divided by values from WT **(Tables 3 & 4)**. The fold values of the DNA content per nuclei relative to WT **(table 4)** are represented as bar graphs in **figure 19.** Interestingly, these results show that the salivary glands from nearly all Mcm10 mutant strains contained higher levels of DNA content per nuclei compared to WT. As shown in **tables 3 and 4**, it was found that the DNA content per nucleus was about 1.5 times to 6.4 times higher in all mutant strains (except strain E451K) than in WT. This suggests that DNA was over-replicated in the salivary glands of the Mcm10 mutant strains.

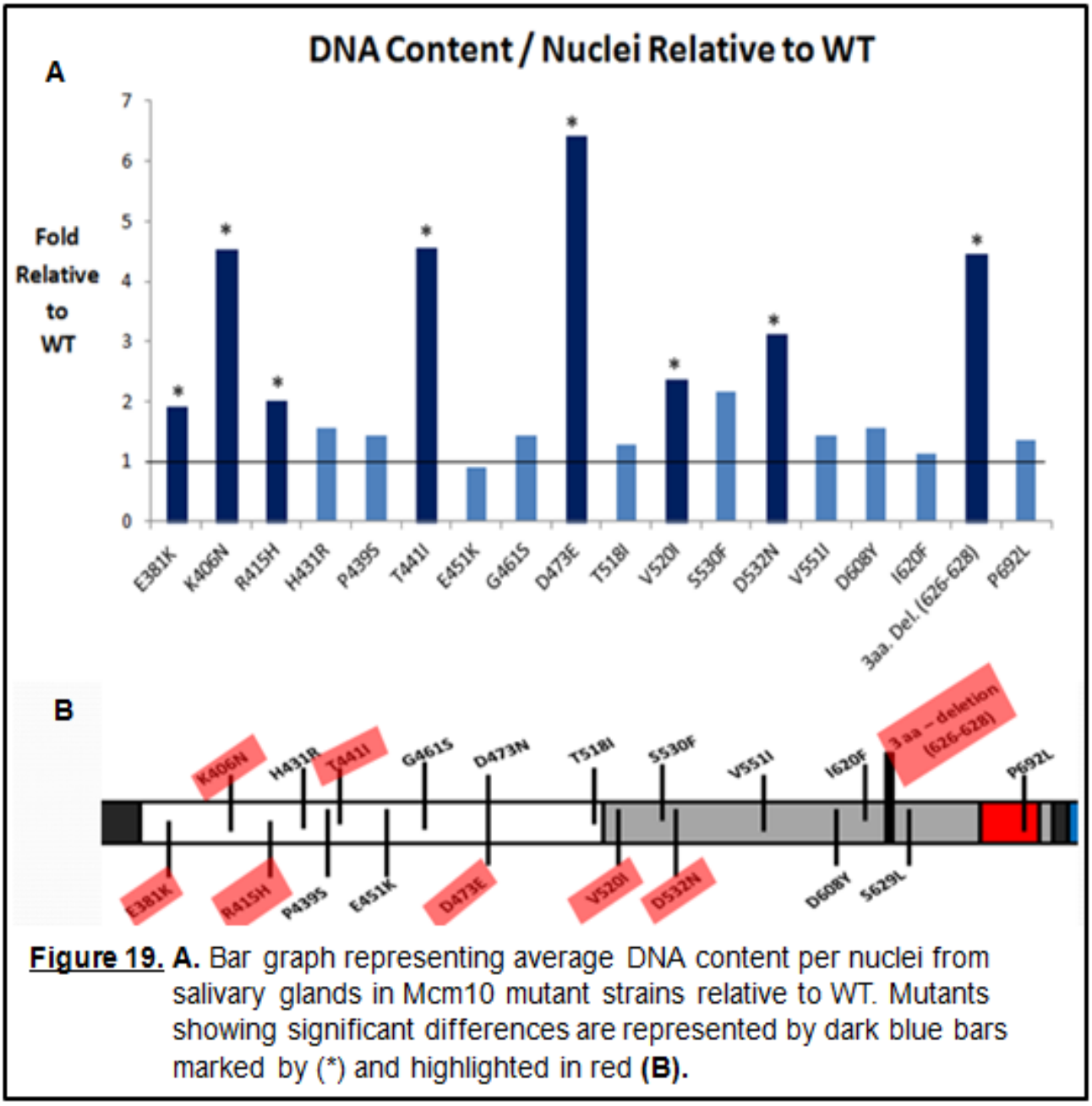

Figure 19. A. Bar graph representing average DNA content per nuclei from salivary glands in Mcm10 mutant strains relative to WT. Mutants showing significant differences are represented by dark blue bars marked by (*) and highlighted in red **(B).**

The DNA content per nuclei was divided by the volume of nuclei of the salivary glands to generate a DNA packing ratio. The results relative to WT are graphed in **figure 20**. If a mutant strain showed significant difference in one or more of the three aspects of the DNA compaction assay, i.e. volume of nuclei, number of nuclei, or DNA content per gland pair, the packing ratio for that respective mutant strain was considered significantly different compared to WT **(Figure 20,** dark blue bars**)**. The results reveal that majority of the Mcm10 mutant strains showed higher DNA packing ratios compared to WT. Interestingly, the number of nuclei in most of the mutants was lower than in WT (except T441I), while the volume of these nuclei varied compared to WT. The high amount of DNA in these strains seems to be packed more tightly as shown by the high packing ratio values relative to WT. For instance, strain D473E had a packing ratio nearly 5.2 times higher than WT and a DNA content per nucleus over 6 times higher than WT. From the data presented in tables 3 and 4 it is evident that Mcm10 mutant alleles in this study have a significant impact on the replication of DNA during the S-phase causing over-replication of DNA.

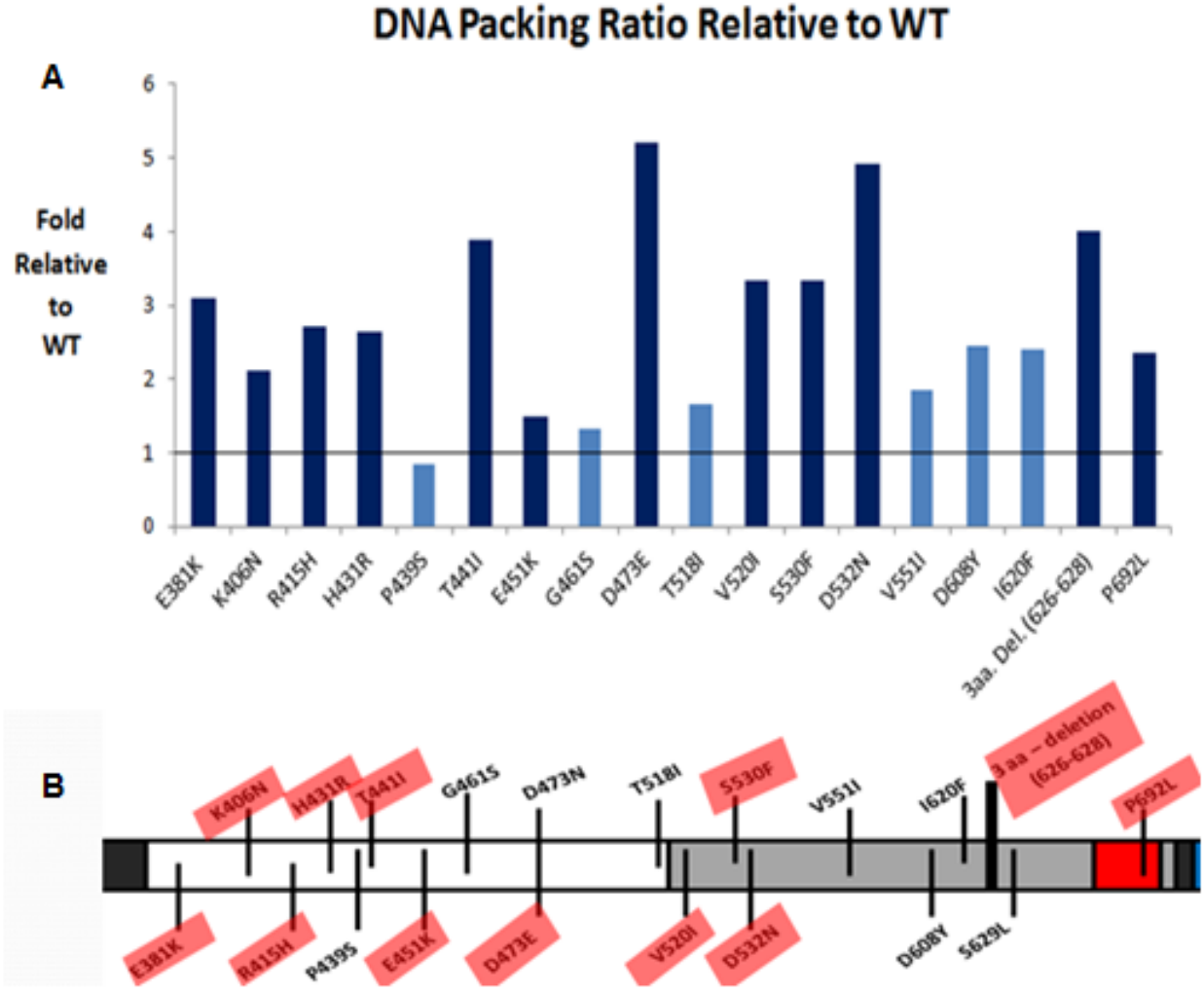

Figure 20. A. Bar graph representing the DNA packing ratio from salivary glands in Mcm10 mutant strains relative to WT. Mutants showing significant differences are represented by dark blue bars and highlighted in red **(B).**

IV. DISCUSSION

In this study we observed that the larval brain cells in *Drosphila* show no M-phase delays but interestingly, all the Mcm10 mutant strains presented with highly defective chromosomal phenotypes during mitosis. The type of defects which include chromosome condensation defects, aneuploidy, anaphase bridge defects, separated sister chromatids and chromosome breaks were all observed in different frequencies in all the mutant strains when compared to WT. Additionally, analysis of the salivary gland tissues revealed that the DNA was over-replicated in nearly all Mcm10 mutant strains and this DNA was also packaged more tightly within each nuclei when compared to WT.

Despite its early discovery along with Mcm 2-7 proteins, Mcm10's function still remains unclear. As one of the first proteins to load after pre-RC assembly, Mcm10 is required for loading downstream proteins and subsequent events in DNA replication initiation. Work over the past decade has established Mcm10 as an essential DNA replication factor that is highly conserved among eukaryotes, and that it is shown to interact with several replication initiation and elongation factors such as ORC **[Izumi *et al.,* 2000],** Mcm 2-7, Pol-α **[Chattopadhyay *et al.,* 2007 and Ricke *et al.,* 2004, 2006]**, RecQ4 helicase **[Xu *et al.*, 2009]**, and And-1 **[Zhu *et al.,* 2007]**. Three structural domains for Mcm10 have been established as the NTD, ID and CTD. The coiled-coil helix within the NTD allows Mcm10 to self-associate **[Du W. *et al.,* 2013]** and this dimerization of Mcm10 could help facilitate its interaction with both the leading and the lagging strands of DNA along with other DNA replication proteins. Mcm10's interactions with ssDNA and Pol-α have shown to be mediated by the conserved ID and CTD **[Robertson *et al.,* 2008].** A recent study has shown that the

binding of Mcm10 to DNA is regulated by a nicotinamide adenine dinucleotide (NAD)-dependent acetylase, SIRT1in human cells **[Fatoba S.T. *et al.,* 2013]**. Both the ID and the CTD of Mcm10 are acetylated in human cells at the lysine residues and some of these get deacetylated by SIRT1 allowing Mcm10 to bind DNA **[Fatoba S.T. *et al.,* 2013].** In addition to modulating Mcm10 for DNA-binding, deacetylation by SIRT1 could also unprotect lysine residues that are otherwise ubiquitinated marking Mcm10 for degradation **[Fatoba S.T. *et al.,* 2013]**. This regulation of Mcm10's binding to DNA by SIRT1 is interesting in that despite the presence of many lysine residues within the NTD, the NTD is not acetylated and is not involved in DNA binding **[Fatoba S.T. *et al.,* 2013]**. This reinforces the notion that the CTD of Mcm10 is crucial in performing additional functions in metazoans and is hence also the site for Mcm10's regulation.

Although the highly conserved ID of Mcm10 has been studied extensively, little is known about the function of the CTD which is an added region unique to higher eukaryotes. The CTD domain of Mcm10 in *Drosophila* was investigated in this study by examining the defects in DNA replication, chromosome segregation and chromosome condensation of the Mcm10 homozygous mutant strains. Previous work conducted by Apger *et al.* showed that a collection of Mcm10 mutants different from those examined in this study, presented with lower fraction of cells in mitosis compared to WT in the larval brain cells of *Drosophila*. Interestingly, no such results were observed in any of the 20 Mcm10 mutant strains used in our study **(Figure 13)**. Of the 20 mutations in the CTD of Mcm10, strains E451K, D473E and S530F showed a large variation in the fraction of cells in mitosis. However, none the Mcm10 mutants presented with any significant delays in progression through the M-phase. A reason

for this could be that Mcm10 is shown to be proteolysed during G2/M phase **[Kaur M. *et al.,* 2010]** and hence the CTD does not affect progression of the M-phase of the cell cycle.

However, the CTD of Mcm10 has been shown to be important in the cell-cycle regulation of Mcm10. The CTD of human Mcm10 has been shown to contain signals for Mcm10's proteolysis during M-phase **[Kaur *et al.,* 2010]**. M-phase proteolysis of Mcm10 is a vital mechanism to prevent aberrant initiation of replication. Work by Kaur *et al.* showed that cells in prophase, metaphase, anaphase, and telophase appeared to lack Mcm10, while cells in interphase expressed the Mcm10 protein. And in this study we observed that the larval brain cells in *Drosphila* do not show any delays in M-phase.

Based on the results in studies conducted by **Xu *et al.* (2009)** it has been shown that Mcm10 plays an inhibitory role in regulating the helicase activity of RecQ4 in G_1 and S phases. Mcm10 is further required for RecQ4's interaction with Mcm2-7 and GINS. Its regulatory role may be controlled by phosphorylation of RecQ4-mediated unwinding of DNA **[Xu e*t al.,* 2009]**. Hence, is appears that the sequestration of RecQ4 by Mcm10 can prevent unlicensed initiation of DNA replication by preventing RecQ4-mediated unwinding of DNA. The regulatory interactions of these two proteins may be reflected in the fact that mutations in each protein results in at least some related chromosome function defects. Studies conducted in *recq4*-deficient mice have shown phenotypes ranging from aneuploidy to slow cell growth **[Hoki *et al*, 2003; Mann *et al*, 2005]**. Similarly, selected Mcm10 mutant strains in our study characteristically also show aberrant chromosome phenotypes including aneuploidy. Mutant strains P439S and D532N showed 10% and 24% aneuploidy chromosomes, respectively **(Figure 15)**. Based on the correlated phenotypes, one might

predict that the sites of these two mutations on Mcm10 could be the regions where RecQ4 may possibly be interacting with Mcm10.

Similarly, chromosome segregation defects such as anaphase bridge defects and separated sister chromatids were also displayed in the Mcm10 mutants. Mcm10 interacts with the cohesion protein And-1/Ctf4 and together have to shown to load DNA Pol-α onto the chromatin **[Zhu W. *et al.,* 2007]**. Ctf4 mutants in *S. cerevisiae* exhibit chromosome missegregation and defects in sister-chromatid cohesion [**Hanna et al. 2001; Mayer et al. 2004; Petronczki et al. 2004**]. Mcm10 interacts with both RecQ4 and And-1/Ctf4 during the process of replication in the S-phase and it is possible that these interactions are affected in the Mcm10 mutants, which could have led to the defective chromosome morphology observed during M-phase. However, validation of this plausible explanation would require further investigation.

High levels of condensation defects were also observed in the Mcm10 mutant strains' brain cells. Since about 10% of mitotic figures in WT were categorized as having condensation defect **(Table 2)** it could be that these chromosomes may have been caught during late G2 phase or early prophase when the chromatin is still in the process of condensing into chromosomes. Hence, there could be two possibilities as to why we see significantly higher frequency of condensation defect in all the Mcm10 mutant strains compared to WT; either, the mitotic figures could have been captured during early prophase suggesting that there could have been a prolonged prophase stage in the mutants, or Mcm10 could have a bona fide role in packaging of the chromatin during mitosis. In either case, the high frequency of condensation defects in all of the Mcm10 mutants points to the idea that

the CTD of Mcm10 could potentially have roles in the segregation and packaging of chromosome during M-phase.

In order to investigate the role of Mcm10 in endoreplication and DNA compaction we conducted experiments using the large polytene salivary glands. We observed that the DNA content per nucleus was significantly higher in several Mcm10 mutants when compared to WT **(Tables 3 and 4)**. The DNA content per nucleus in strains K406N, T441I, D473E and the 3aa. deletion was observed to be 4 to 6 times higher than in the nuclei from WT. This clearly shows that DNA was over-replicated in the salivary glands of Mcm10 mutant strains and suggests that Mcm10 plays a crucial role in regulating replication of DNA in endocycling cells as well. Additionally, even though the number and volume of the nuclei varied in these mutants, the high levels of DNA content resulted in a greater DNA packaging ratio of all Mcm10 mutants compared to WT. These results are very interesting in that, even though the DNA content was much higher in the Mcm10 mutant strains, the cells were able to package all of it in the nuclei. This suggests that either the cells (or nuclei) have considerable excess of all the constituents of chromatin or that increase in DNA content resulted in increased production of all the components required for chromatin packaging. In addition to helping understand some aspects of Mcm10's role in replication these results could also aid in understanding the regulatory interactions between DNA and genes required for synthesis of chromatin constituents. These results suggest that Mcm10 is involved in replication of DNA even in endocycling cells. Mutation in the CTD of Mcm10 resulted in over-replication of DNA which in turn resulted in highly compacted packaging of DNA within the nuclei of the salivary tissue. Studies over the last two decades have shown that while mitotic functions are repressed in the endocycle, many of the proteins required for DNA replication and the

regulation of G1-S phase are shared between the mitotic cycle and the endocycle **[Edgar and Orr-Weaver, 2001; Lee and Orr-Weaver, 2003**]. Although needed for replication in cells undergoing normal cell cycle, *orc1* is shown to be dispensable in endoreplication in *Drosophila.* However, other essential components such as Dup/cdt1 and Mcm2-7 needed in replication of normal cells are also required for endoreplication **[Park & Asano, 2008]**. And in this study we show that in addition to being an essential DNA replication factor in normal cells, *Drosophila* Mcm10 also plays a role in DNA replication in endocycling cells.

Mcm10 is a crucial player in orchestrating the licensing and activation of the pre-RC during replication initiation. With studies revealing more and more information about the structure of Mcm10 and its interactions with DNA and other proteins, it is slowly shedding light on some aspects of the functionality of Mcm10. Mcm10 seems to be a scaffolding protein that uses different regions of its structure to coordinate interactions with various proteins and DNA during replication. The self-association through its NTD can allow Mcm10 to interact with both the leading and lagging strands of DNA via binding through its ID and CTD.

Mcm10 Mutant Strain	Mitotic Chromosome Phenotypes Compared to WT						Salivary Gland DNA Compaction Analysis Compared to WT				
	Normal Mitotic Figure	Condensation Defect	Aneuploidy	Anaphase Bridge Defect	Separated Sister Chromatids	Other Defect	Volume of Nuclei	# of Nuclei Per Gland pair	DNA Content Per Gland Pair	DNA Per Nuclei	Packing Ratio (DNA Compaction)
E381K	-	+*	+	-	-	+	-	-*	+*	+	+
K406N	-*	+*	+	-	+	+*	+*	-*	+*	+	+
R415H	-*	+*	+	+	+	+	-	-	+*	+	+
H431R	-*	+*	=	-	+	+	-*	-*	+	+	+
P439S	-*	+*	+	+	+	+	+	-	+	+	-
T441I	-*	+*	+	+	+	+*	+	+	+*	+	+
E451K	-*	+	+	+*	+	+*	-*	-	+	-	+
G461S	-*	+*	+	+	-	-	+	-	+	+	+
D473N	-*	+*	+	+	-	-	n/a	n/a	n/a	n/a	n/a
D473E	-*	+	+	+	+	+	+	-*	+*	+	+
T518I	-*	+*	=	-	+	+	-	-	-	+	+
V520I	-*	+	=	+	-	+	-*	-*	+*	+	+
S530F	-*	+	+	+	+	+*	-	-*	+	+	+
D532N	-*	+	+	+	-	+	-	-*	+*	+	+
V551I	-*	+*	=	+	+	+	-	-	+	+	+
D608Y	-*	+*	=	-	+	-	-	-	+	+	+
I620F	-*	+*	+	+	+*	+	-*	-	+	+	+
3aa. Del. (626-628)	-*	+*	+	+	-	+	+	-	+*	+	+
S629L	-*	+*	+	+	-	+*	n/a	n/a	n/a	n/a	n/a
P692L	-*	+*	=	+*	+	+	-*	-	+	+	+

Table 5. Summary of the data compiled from assays performed on all Mcm10 mutants compared to WT. **(-)** represents values lower than WT and **(+)** represents values greater than WT. Significant differences compared to WT are represented in red, **(-*)** denoted for lower and **(+*)** denoted for values greater than WT. **(=)** represents values equivalent to WT. DNA compaction analyses were not performed on strains D473N and S629L and so data values are represented as (n/a).

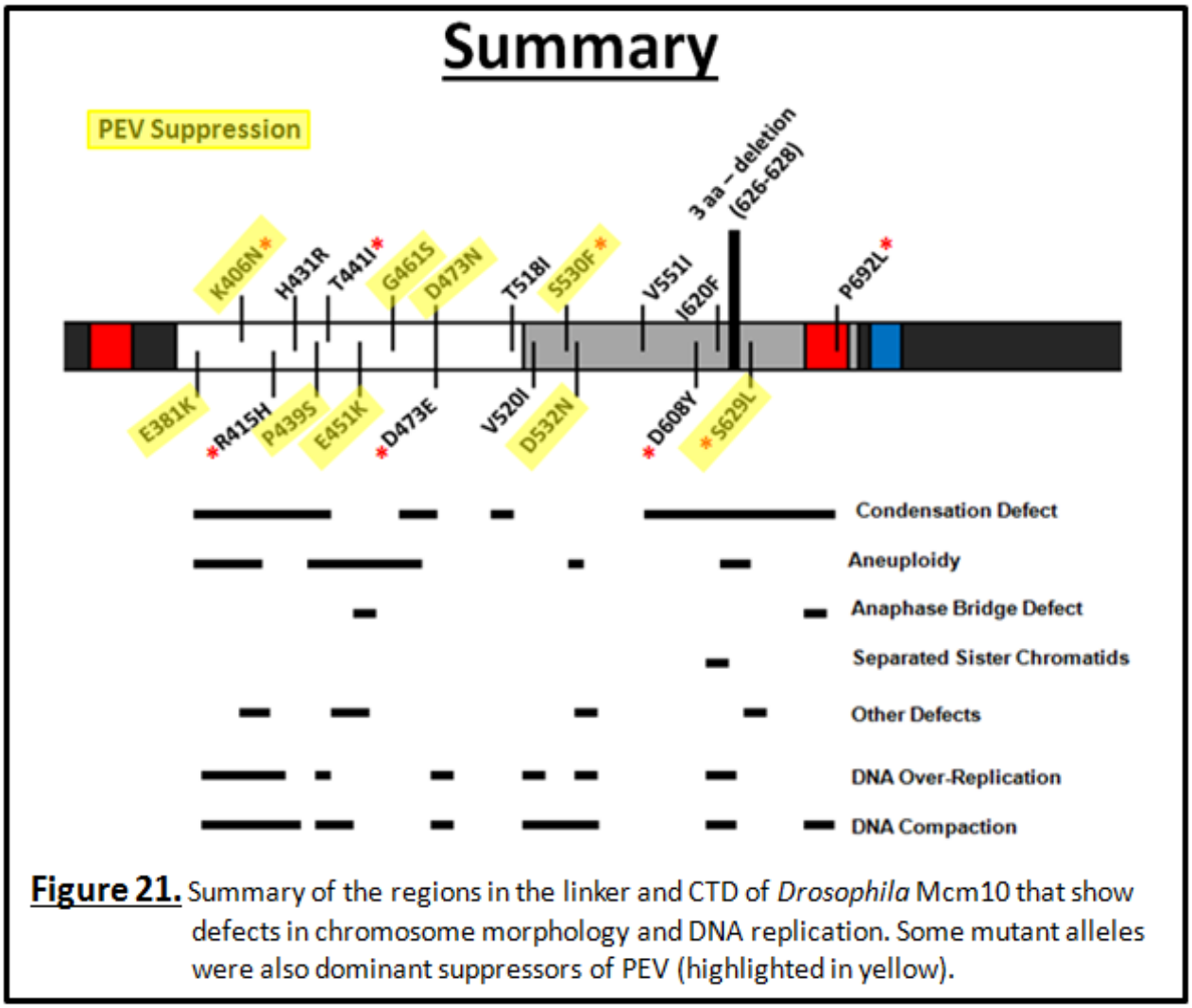

Figure 21. Summary of the regions in the linker and CTD of *Drosophila* Mcm10 that show defects in chromosome morphology and DNA replication. Some mutant alleles were also dominant suppressors of PEV (highlighted in yellow).

Based on the data from this study we have schematically mapped regions on the CTD of *Drosophila* Mcm10 where the various defects in DNA replication and chromosome morphology were observed during the S- and M-phases of the cell **(Figure 21)**. As depicted in **figure 21** and **table 5**, mutations in different regions of the CTD manifested different levels and types of defects in chromosome morphology such as condensation defects, aneuploidy, anaphase bridge defect, and separated sister

chromatids. It can be seen that defects in certain regions of the CTD also resulted in significant over-replication of DNA in endocycling cells, which led to tightly packed DNA. In addition, previously conducted work on PEV analysis shows that some of the Mcm10 mutant strains **(Figure 21**, highlighted in yellow**)** from the collection used in this study suppress PEV and this suggests that certain regions of the CTD are also involved in heterochromatin formation.

From the data presented in this study along with the PEV results we show that the function of Mcm10 in DNA replication and its role in defining chromosome morphology are separable. For instance, mutant strains E451K, G461S, V551I, D608Y and I620F show defective chromosome phenotypes but do not show significantly higher DNA content **(Table 5 and Figure 21)** showing that roles of Mcm10 are separable. In addition, mutant strain P692L did not contain significantly over-replicated DNA compared to WT during S-phase. However, the DNA was packaged more tightly and severe chromosome condensation defects were observed in this mutant strain. Hence, it can be inferred from this data that the high frequencies of condensation defects observed in the mutant strains were a result of Mcm10's bona fide role in chromatin packaging and that this defect was not due a prolonged prophase during mitosis.

Furthermore, the result that defects in the CTD of Mcm10 led to over-replication is quite interesting since endoreplication has been used as a default program upon mitotic catastrophe in many cancer cells **[Storchova and Pellman 2004]**. Mcm10 has been found to be frequently over-expressed in many types of cancers and since Mcm10 partners with RecQ4 and binds to Mcm2-7 complex activating its helicase activity it suggests that Mcm10 plays a critical role in tumor progression as well **[Das M**

***et al.,* 2013]**. Owing to its role critical role in DNA replication along with its possible roles in maintaining chromatin morphology as shown in this study, Mcm10 presents itself as a prime target that gets destructed in order to disrupt the replication machinery in cancers.

In conclusion, a summary of our results provide evidence that Mcm10 has roles in DNA endoreplication, mediation of chromosome morphology, and M-phase chromosome segregation. Additionally, the involvement of different regions of Mcm10 in performing these different functions points towards the structural importance of the unique CTD which has evolved to take on added roles that may be required during the complex developmental processes of metazoans. Data in this study have helped shed some more light on additional roles of Mcm10 a protein which is so essential that aberrant expression of this key replication factor has found its place as one of the top ten cancer associated proteins **[Wu *et al.,* 2012]**. Hence, continuing to understand Mcm10's role at the molecular level will not just appease the scientific curiosity of unraveling how yet another protein is involved in carrying out replication and maintaining other chromatin associated functions but it could also prove to be an essential target in developing therapeutic drugs in cancer treatment.

V. REFERENCES

Apger, Jennifer, et al. "Multiple Functions for Drosophila Mcm10 Suggested through Analysis of Two Mcm10 Mutant Alleles." *Genetics* 185.4 (2010): 1151-U44.

Bell, SP, and A. Dutta. "DNA Replication in Eukaryotic Cells." *Annual Review of Biochemistry* 71 (2002): 333-74.

Campbell L, N. B. and J. A. Reece. 2002. Biology, 7th Ed. Benjamin Cummings, San Fransico, CA.

Chang, CC, et al. "Nuclear and Microtubule Dynamics of G(2)/M Somatic Nuclei during Haploidization in Germinal Vesicle-Stage Mouse Oocytes." *Biology of reproduction* 70.3 (2004): 752-8.

Chattopadhyay, Sharbani, and Anja-Katrin Bielinsky. "Human Mcm10 Regulates the Catalytic Subunit of DNA Polymerase-Alpha and Prevents DNA Damage during Replication." *Molecular biology of the cell* 18.10 (2007): 4085-95.

Chmielewski, J.P. Henderson L, Smith CM, Christensen TW. “Drosophila Psf2 has a role in chromosome condensation.” *Chromosoma*. (2012);121(6):585-96

Chmielewski, J. P., and Tim W. Christensen. “Novel method for determining chromosome compaction and DNA content of salivary gland nuclei in Drosophila”*. Dros. Inf. Serv*. (2011): 94.

Christensen, TW, and BK Tye. "Drosophila Mcm10 Interacts with Members of the Prereplication Complex and is Required for Proper Chromosome Condensation." *Molecular biology of the cell* 14.6 (2003): 2206-15.

Cook, CR, et al. "A Novel Zinc Finger is Required for Mcm10 Homocomplex Assembly." *Journal of Biological Chemistry* 278.38 (2003): 36051-8.

Das, Mitali, et al. "Over Expression of Minichromosome Maintenance Genes is Clinically Correlated to Cervical Carcinogenesis." *Plos One* 8.7 (2013): e69607

Das-Bradoo, S., RM Ricke, and AK Bielinsky. "Interaction between PCNA and Diubiquitinated Mcm10 is Essential for Cell Growth in Budding Yeast." *Molecular and cellular biology* 26.13 (2006): 4806-17.

Di Perna, Roberta, et al. "The Physical Interaction of Mcm10 with Cdc45 Modulates their DNA-Binding Properties." *Biochemical Journal* 454 (2013): 333-43.

Douglas, NL, SK Dozier, and JJ Donato. "Dual Roles for MCM10 in DNA Replication Initiation and Silencing at the Mating-Type Loci." *Molecular biology reports* 32.4 (2005): 197-204.

Du W, Stauffer ME, Eichman BF. “Structural Biology of Replication Initiation Factor Mcm10.” *Subcell Biochem.* (2012):62;197-216.

Du W, Josephrajan A, Adhikary S, Bowles T, Bielinsky AK, and Eichman BF. “Mcm10 self-association is mediated by an N-terminal coiled-coil domain.” *Plos One* (2013)

Edgar, BA, and TL Orr-Weaver. "Endoreplication Cell Cycles: More for Less." *Cell* 105.3 (2001): 297-306.

Eisenberg, Shlomo, et al. "Novel DNA Binding Properties of the Mcm10 Protein from Saccharomyces Cerevisiae." *Journal of Biological Chemistry* 284.37 (2009): 25412-20.

Fatoba, Samuel T., et al. "Human SIRT1 Regulates DNA Binding and Stability of the Mcm10 DNA Replication Factor Via Deacetylation." *Nucleic acids research* 41.7 (2013): 4065-79.

Feger, G., et al. "Dpa, a Member of the Mcm Family, is Required for Mitotic Dna-Replication but Not Endoreplication in Drosophila." *Embo Journal* 14.21 (1995): 5387-98.

Fien, K., et al. "Primer Utilization by DNA Polymerase Alpha-Primase is Influenced by its Interaction with Mcm10p." *Journal of Biological Chemistry* 279.16 (2004): 16144-53.

Fien, Karen, and Jerard Hurwitz. "Fission Yeast Mcm10p Contains Primase Activity." *Journal of Biological Chemistry* 281.31 (2006): 22248-60.

Fox, Donald T., and Robert J. Duronio. "Endoreplication and Polyploidy: Insights into Development and Disease." *Development* 140.1 (2013): 3-12.

Fu, Yu V., et al. "Selective Bypass of a Lagging Strand Roadblock by the Eukaryotic Replicative DNA Helicase." *Cell* 146.6 (2011): 930-40.

Gambus, A., et al. "GINS Maintains Association of Cdc45 with MCM in Replisome Progression Complexes at Eukaryotic DNA Replication Forks." *Nature cell biology* 8.4 (2006): 358-U41.

Gillespie, PJ, and T. Hirano. "Scc2 Couples Replication Licensing to Sister Chromatid Chromatid in Xenopus Egg Extracts." *Current Biology* 14.17 (2004): 1598-603.

Gregan, J., et al. "Fission Yeast Cdc23/Mcm10 Functions After Prereplicative Complex Formation to Promote Cdc45 Chromatin Binding." *Molecular biology of the cell* 14.9 (2003): 3876-87.

Hanna, JS, et al. "Saccharomyces Cerevisiae CTF18 and CTF4 are Required for Sister Chromatid Cohesion." *Molecular and cellular biology* 21.9 (2001): 3144-58.

Heller, Ryan C., et al. "Eukaryotic Origin-Dependent DNA Replication in Vitro Reveals Sequential Action of DDK and S-CDK Kinases." *Cell* 146.1 (2011): 80-91.

Henikoff S. “Position-effect Variegation After 60 Years.” *Trends in Genetics*. 12 (1990):422-6.

Hoki, Y., et al. "Growth Retardation and Skin Abnormalities of the Recq/4-Deficient Mouse." *Human molecular genetics* 12.18 (2003): 2293-9.

Homesley, L., et al. "Mcm10 and the MCM2-7 Complex Interact to Initiate DNA Synthesis and to Release Replication Factors from Origins." *Genes & development* 14.8 (2000): 913-26.

Im, Jun-Sub, et al. "Assembly of the Cdc45-Mcm2-7-GINS Complex in Human Cells Requires the Ctf4/And-1, RecQL4, and Mcm10 Proteins." *Proceedings of the National Academy of Sciences of the United States of America* 106.37 (2009): 15628-32.

Izumi, M., et al. "The Human Homolog of Saccharomyces Cerevisiae Mcm10 Interacts with Replication Factors and Dissociates from Nuclease-Resistant Nuclear Structures in G(2) Phase." *Nucleic acids research* 28.23 (2000): 4769-77.

Kanke, Mai, et al. "Mcm10 Plays an Essential Role in Origin DNA Unwinding After Loading of the CMG Components." *Embo Journal* 31.9 (2012): 2182-94.

Kaur, Manpreet, et al. "Mcm10 Proteolysis Initiates before the Onset of M-Phase." *Bmc Cell Biology* 11 (2010): 84.

Kawasaki, Y., S. Hiraga, and A. Sugino. "Interactions between Mcm10p and Other Replication Factors are Required for Proper Initiation and Elongation of Chromosomal DNA Replication in Saccharomyces Cerevisiae." *Genes to Cells* 5.12 (2000): 975-89.

Kondorosi, E., F. Roudier, and E. Gendreau. "Plant Cell-Size Control: Growing by Ploidy?" *Current opinion in plant biology* 3.6 (2000): 488-92.

Lake, Cathleen M., et al. "A Genetic Analysis of the Drosophila mcm5 Gene Defines a Domain Specifically Required for Meiotic Recombination." *Genetics* 176.4 (2007): 2151-63.

Lee, Chanmi, et al. "Alternative Mechanisms for Coordinating Polymerase Alpha and MCM Helicase." *Molecular and cellular biology* 30.2 (2010): 423-35.

Lee, Hyun O., Jean M. Davidson, and Robert J. Duronio. "Endoreplication: Polyploidy with Purpose." *Genes & development* 23.21 (2009): 2461-77.

Lee, JK, YS Seo, and J. Hurwitz. "The Cdc23 (Mcm10) Protein is Required for the Phosphorylation of Minichromosome Maintenance Complex by the Dfp1-Hsk1 Kinase." *Proceedings of the National Academy of Sciences of the United States of America* 100.5 (2003): 2334-9.

Lee, LA, and TL Orr-Weaver. "Regulation of Cell Cycles in Drosophila Development: Intrinsic and Extrinsic Cues." *Annual Review of Genetics* 37 (2003): 545-78.

Lei, M., et al. "Mcm2 is a Target of Regulation by Cdc7-Dbf4 during the Initiation of DNA Synthesis." *Genes & development* 11.24 (1997): 3365-74.

Liachko, I., and BK Tye. "Mcm10 is Required for the Maintenance of Transcriptional Silencing in Saccharomyces Cerevisiae." *Genetics* 171.2 (2005): 503-15.

Liachko, Ivan, and Bik K. Tye. "Mcm10 Mediates the Interaction between DNA Replication and Silencing Machineries." *Genetics* 181.2 (2009): 379-91.

Lilly, MA, and RJ Duronio. "New Insights into Cell Cycle Control from the Drosophila Endocycle." *Oncogene* 24.17 (2005): 2765-75.

Lilly, MA, and AC Spradling. "The Drosophila Endocycle is Controlled by Cyclin E and Lacks a Checkpoint Ensuring S-Phase Completion." *Genes & development* 10.19 (1996): 2514-26.

Liu, Yuan, Thomas A. Richards, and Stephen J. Aves. "Ancient Diversification of Eukaryotic MCM DNA Replication Proteins." *Bmc Evolutionary Biology* 9 (2009): 60.

Machida, YJ, JL Hamlin, and A. Dutta. "Right Place, Right Time, and Only Once: Replication Initiation in Metazoans." *Cell* 123.1 (2005): 13-24.

Maines, JZ, et al. "Drosophila dMyc is Required for Ovary Cell Growth and Endoreplication." *Development* 131.4 (2004): 775-86.

Mann, MB, et al. "Defective Sister-Chromatid Cohesion, Aneuploidy and Cancer Predisposition in a Mouse Model of Type II Rothmund-Thomson Syndrome." *Human molecular genetics* 14.6 (2005): 813-25.

Mayer, ML, et al. "Identification of Protein Complexes Required for Efficient Sister Chromatid Cohesion." *Molecular biology of the cell* 15.4 (2004): 1736-45.

Merchant, AM, et al. "A Lesion in the DNA Replication Initiation Factor Mcm10 Induces Pausing of Elongation Forks through Chromosomal Replication Origins in Saccharomyces Cerevisiae." *Molecular and cellular biology* 17.6 (1997): 3261-71.

Moseley, James B., et al. "A Spatial Gradient Coordinates Cell Size and Mitotic Entry in Fission Yeast." *Nature* 459.7248 (2009): 857-U8.

Moyer, Stephen E., Peter W. Lewis, and Michael R. Botchan. "Isolation of the Cdc45/Mcm2-7/GINS (CMG) Complex, a Candidate for the Eukaryotic DNA Replication Fork Helicase." *Proceedings of the National Academy of Sciences of the United States of America* 103.27 (2006): 10236-41.

Nurse, P. "A Long Twentieth Century of the Cell Cycle and Beyond." *Cell* 100.1 (2000): 71-8.

Okorokov, Andrei L., et al. "Hexameric Ring Structure of Human MCM10 DNA Replication Factor." *EMBO reports* 8.10 (2007): 925-30.

Osborn, A. J., S. J. Elledge, and L. Zou. "Checking on the Fork: The DNA-Replication Stress-Response Pathway." *Trends in cell biology* 12.11 (2002)

Pauline C. Ng and Henikoff S. “SIFT: predicting amino acid changes that affect protein function.” *Nucleic Acids Research*, 31.13 (2003): 3812-14.

Park, So Young, and Maki Asano. "The Origin Recognition Complex is Dispensable for Endoreplication in Drosophila." *Proceedings of the National Academy of Sciences of the United States of America* 105.34 (2008): 12343-8.

Petronczki, M., et al. "Sister-Chromatid Cohesion Mediated by the Alternative RF-C-Ctf18/(Dcc1)/(Ctf8), the Helicase Chl1 and the Polymerase-Alpha-Associated Protein Ctf4 is Essential for Chromatid Disjunction during Meiosis II." *Journal of cell science* 117.16 (2004): 3547-59.

Remus, Dirk, et al. "Concerted Loading of Mcm2-7 Double Hexamers Around DNA during DNA Replication Origin Licensing." *Cell* 139.4 (2009): 719-30.

Ricke, RM, and AK Bielinsky. "A Conserved Hsp10-Like Domain in Mcm10 is Required to Stabilize the Catalytic Subunit of DNA Polymerase-Alpha in Budding Yeast." *Journal of Biological Chemistry* 281.27 (2006): 18414-25.

Ricke, RM, and AK Bielinsky. "Mcm10 Regulates the Stability and Chromatin Association of DNA Polymerase-Alpha." *Molecular cell* 16.2 (2004): 173-85.

Robertson, Patrick D., et al. "Solution NMR Structure of the C-Terminal DNA Binding Domain of Mcm10 Reveals a Conserved MCM Motif." *Journal of Biological Chemistry* 285.30 (2010).

Robertson, Patrick D., et al. "Domain Architecture and Biochemical Characterization of Vertebrate Mcm10." *Journal of Biological Chemistry* 283.6 (2008)

Sawyer, S. L., et al. "Mcm10 and Cdc45 Cooperate in Origin Activation in Saccharomyces Cerevisiae." *Journal of Molecular Biology* 340.2 (2004): 195-202.

Sclafani, R. A., and T. M. Holzen. "Cell Cycle Regulation of DNA Replication." *Annual Review of Genetics* 41 (2007): 237-80.

Sheu, Yi-Jun, and Bruce Stillman. "Cdc7-Dbf4 Phosphorylates MCM Proteins Via a Docking Site-Mediated Mechanism to Promote S Phase Progression." *Molecular cell* 24.1 (2006): 101-13.

Storchova, Z., and D. Pellman. "From Polyploidy to Aneuploidy, Genome Instability and Cancer." *Nature Reviews Molecular Cell Biology* 5.1 (2004): 45-54.

Takahashi, TS, et al. "Recruitment of Xenopus Scc2 and Cohesin to Chromatin Requires the Pre-Replication Complex." *Nature cell biology* 6.10 (2004): 991

Tanaka, Seiji, et al. "CDK-Dependent Phosphorylation of Sld2 and Sld3 Initiates DNA Replication in Budding Yeast." *Nature* 445.7125 (2007): 328-32.

Thu, Yee Mon, and Anja-Katrin Bielinsky. "Enigmatic Roles of Mcm10 in DNA Replication." *Trends in biochemical sciences* 38.4 (2013): 184-94.

van Deursen, Frederick, et al. "Mcm10 Associates with the Loaded DNA Helicase at Replication Origins and Defines a Novel Step in its Activation." *Embo Journal* 31.9 (2012): 2195-206.

Wang, Jiafeng, et al. "Ctf4p Facilitates Mcm10p to Promote DNA Replication in Budding Yeast." *Biochemical and biophysical research communications* 395.3 (2010): 336-41.

Warren, Eric M., et al. "Structural Basis for DNA Binding by Replication Initiator Mcm10." *Structure* 16.12 (2008): 1892-901.

Warren, Eric M. y., et al. "Physical Interactions between Mcm10, DNA, and DNA Polymerase Alpha." *Journal of Biological Chemistry* 284.36 (2009): 24662-72.

Watase, George, Haruhiko Takisawa, and Masato T. Kanemaki. "Mcm10 Plays a Role in Functioning of the Eukaryotic Replicative DNA Helicase, Cdc45-Mcm-GINS." *Current Biology* 22.4 (2012): 343-9.

Wohlschlegel, JA, et al. "Xenopus Mcm10 Binds to Origins of DNA Replication After Mcm2-7 and Stimulates Origin Binding of Cdc45." *Molecular cell* 9.2 (2002): 233-40.

Wu C. et al., “Integrating gene expression and protein-protein interaction network to prioritize cancer-associated genes.” *BMC Bioinformatics*.(2012):13; 182.

Xu, Xiaohua, et al. "MCM10 Mediates RECQ4 Association with MCM2-7 Helicase Complex during DNA Replication." *Embo Journal* 28.19 (2009): 3005-14.

Zegerman, Philip, and John F. X. Diffley. "Phosphorylation of Sld2 and Sld3 by Cyclin-Dependent Kinases Promotes DNA Replication in Budding Yeast." *Nature* 445.7125 (2007): 281-5.

Zhu, Wenge, et al. "Mcm10 and and-1/CTF4 Recruit DNA Polymerase Alpha to Chromatin for Initiation of DNA Replication." *Genes & development* 21.18 (2007): 2288-99.